Università Degli Studi di Roma “La Sapienza”

Facoltà di Ingegneria Civile e Industrial Dipartimento di Meccanica e Aeronautica

Tesi di Dottorato di Ricerca in Ingegneria Industriale e Gestionale

Innovative methods for metal joining

Candidate

Mohammadzadeh Amin

Advisor

Professoressa. Gisario Annamaria

Rome, Italy 2019

Contents

Index of figures

Index of tables

Abstract

In modern technologies, almost all products are fabricated by joining processes. This field is extremely broad, involving many different methods. Although originally developed on an empirical basis, these methods are becoming more dependent on sound scientific and engineering principles to satisfy the needs of advancing materials technology. Indeed, the joining of metals is so important that a modern society could not exist without considerable expertise in this field. Diffusion bonding is a solid state bonding process able to produce components without unexpected microstructure changes and with a minimum of deformation. In diffusion, bonding every parameter has an important effect on the properties of the resulting joints. This PhD study aims to investigate the effect of interlayer, bonding pressure, bonding temperature, and holding time on the diffusion bonding process of stainless steel of grade 316 L and pure copper (99.99 wt.%) to determine the optimum bonding parameters in terms of the resulting mechanical properties (strength and shear strength) of the joints. The experiments were performed at two stages of screening and modification. The samples obtained from the experimental section were examined through the tensile and shear strength tests and analyzed by optical microscope (OM), high resolution scanning electron microscopy (HR-SEM) in back-scattered (BSC) mode, and energy dispersive x-ray spectroscopy (EDS). Consequently, maximum bond tensile and shear strength were achieved with 463.01 MPa and 118.85 Mpa, respectively under 14.03 (Mpa) bonding pressure at 925.21 °C (using nickel interlayer and 30 minutes holding time).

1. Introduction

The metal-joining methods play an important role in modern technologies. Almost all of the industrial products are practically fabricated by joining processes requiring joint integrity. Therefore, joint integrity is as important as component integrity and even more. Generally, the goal of the joining processes is to seamlessly join separate pieces of either different or the same materials together. In conventional metal-joining methods, mechanical fasteners such as bolts or rivets are often employed to join metal components together. There is also another concept to make detached pieces of metals unified which is based on diverse methods such as arc welding, electron beam welding (EBW), laser beam welding (LBW), adhesive bonding, brazing, soldering, explosion bonding, and diffusion bonding [1]. By sufficiently closing the atoms at the edge of one part to the atoms at the edge of another part, the interatomic attraction is developed which leads to unifying two parts together. Although this concept is simple in theoretical view, it is complicated to make it practical. There are several parameters that affect the joint properties such as surface roughness, impurities, fitting imperfections, and the varied characteristics of the materials being joined [1]. When permanent joints between parts are required, these methods are preferred. Chemical and mechanical compatibility of the surfaces of the joining parts have a great importance in joining procedure [1–3]. Several technological approaches have been employed to eliminate contact problems such as protective atmosphere, insertion of an intermediate layer between surfaces, cleaning of the surfaces, fluxing, melting, or coating the joint surfaces. Even when the joining processes are performed successfully, following performance of the joined parts is often limited by structural changes and degradation of engineering properties during the joining processes. Typical joining problems usually consist of preparation of clean surfaces, non-uniform solidification of weld materials, interfacial stress induced by periodic heating and cooling, solid-state inter-diffusion,

undesirable phases and structural formations, creep, corrosion, fracture, and gradual degradation of electrical and mechanical properties in the proximity of the original interface [2,3].

1.1. Joining methods

1.1.1. Arc welding

Arc welding is one of the joining processes, which joins the separated parts utilizing the heat of an electric arc created between the work piece and electrode. Figure 1 illustrates the schematic of this method [4]. As shown in Figure 1, the electrode or filler metal is heated until transferred to liquid state and deposited into the joint to make the weld without need to pressure. The electric circuit is created by closing two electrodes (the electrode and the work piece) and the arc is formed at low voltage, and high current. The electric energy is converted into an arc with intense heat release which creates high temperature (about 5500 ºC).

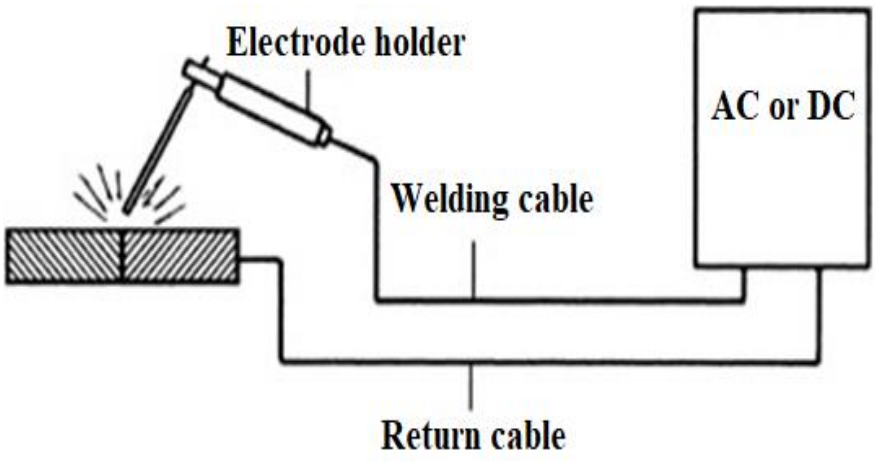

Figure 1. The schematic of arc welding [4]

Despite the popularity of this method, it is associated with couple of disadvantages; firstly, control of temperature is hard, and secondly, production of direct current (DC) and alternative current (AC) requires heavy and expensive rectifiers [4, 5].

1.1.2. Electron beam welding (EBW)

EBW is known as new technology for “clean welds”. As shown in Figure 2 the electrons are directed towards the metals from a tungsten gun which is heated up to 2200 ˚C instead of high velocity of electrons [6, 7]. In other words, electrons are introduced to a magnetic field and centered by the anode and deflecting coils. Using vacuum condition in producing electron beam in this method leads to high purity of formed weld.

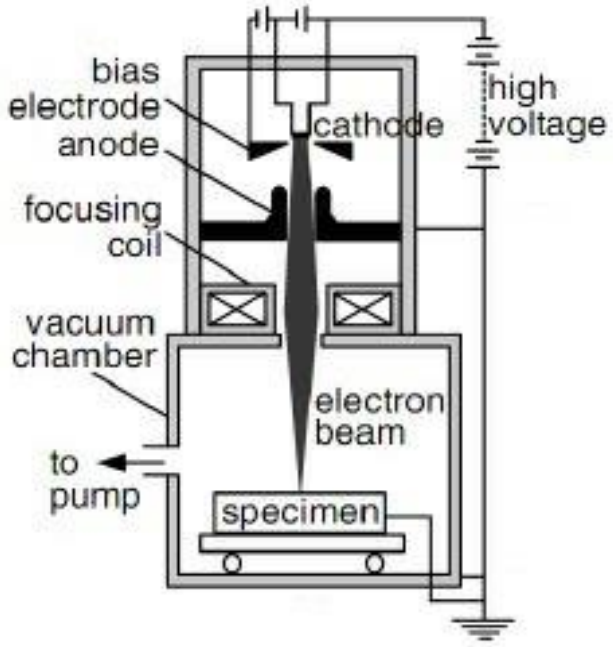

Figure 2. The schematic of electron beam welding

In addition to vacuum condition, low heat input, low distortion, narrow heat affected zone (HAZ) are other influential parameters in high purity of weld [8]. The most important drawback of this method is shrinkage of the melted materials during cooling after solidification, which may result in unwanted phenomena such as cracking, deformation and changes in shape.

1.1.3. Laser Beam Welding (LBW)

LBW is a fusion welding process that is performed by means of heat energy of a highly concentrated, coherent light beam focusing on the joint of the two separated parts, which are required to be welded to each other (Figure 3) [10]. Advantages of the LBW welds are high quality, deep penetrated, and exhibit narrow of HAZ [10]. The benefits of LBW over EBW are removing vacuum chamber, no x-rays emission, and focusing and directing of laser beams on the target by optical lenses and mirrors [10].

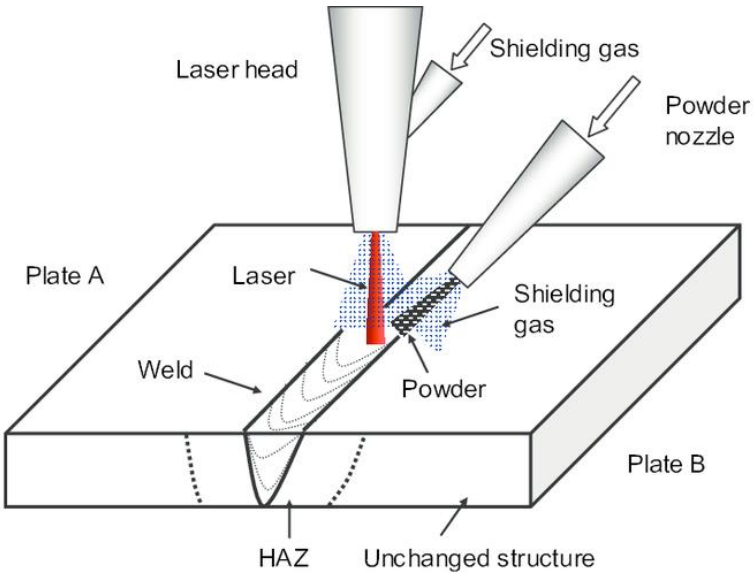

Figure 3. The schematic of the laser beam welding [10]

Despite the benefits, this method has, it can be used for the samples with thickness of less than 19 mm [10]. Hence, due to the highly concentrated energy, which is located in the small area of the laser beam, only small parts can be joined by LBW. In other words, the success of LBW is highly dependent on the operator's skill to choose the appropriate welding parameters [11].

1.1.4. Adhesive bonding

Adhesive bonding is a wafer bonding approach in which an intermediate layer is applied to connect substrates of different types of materials. Adhesive bonding benefits from relatively low bonding temperature as well as the absence of electric voltage and current. In this method use of different substrates such as silicon, glass, metals and other semiconductor materials is possible since the wafers do not contact directly [12]. The most significant shortage of this process is expansion of the small structures during patterning which obstructs the production of an accurate intermediate layer with precise dimension control. Another disadvantage lies in the possibility of corrosion caused by out-gassed products, thermal instability and moisture penetration, which make this method unreliable [12]. Another drawback is that hermetically sealed encapsulation is not possible due to higher gas and water molecules permeability while using organic adhesives [13,14].

1.1.5. Brazing

Joining the separated parts in brazing method is performed by the capillary action of the melted filler metal between the faying (contact) surfaces of the metal parts as shown in Figure 4. In this method, the filler metal has a melting temperature (liquidus) in the range of 450°C up to 800 °C, but below the melting point (solidus) of base metals to be joined; therefore, only the filler is melted and the base material does not melt [15]. Economical fabrication of complex and multicomponent assemblies, simplicity, ability to

join various materials with different thicknesses, and the ability of joining a large variety of dissimilar metals are some of the advantages of brazing method. Despite the abovementioned advantages, this method suffers from many limitations. The most significant drawback of this process is heterogeneity of the bond, which leads to a brazed joint composed of different phases with various physical and chemical properties [15].

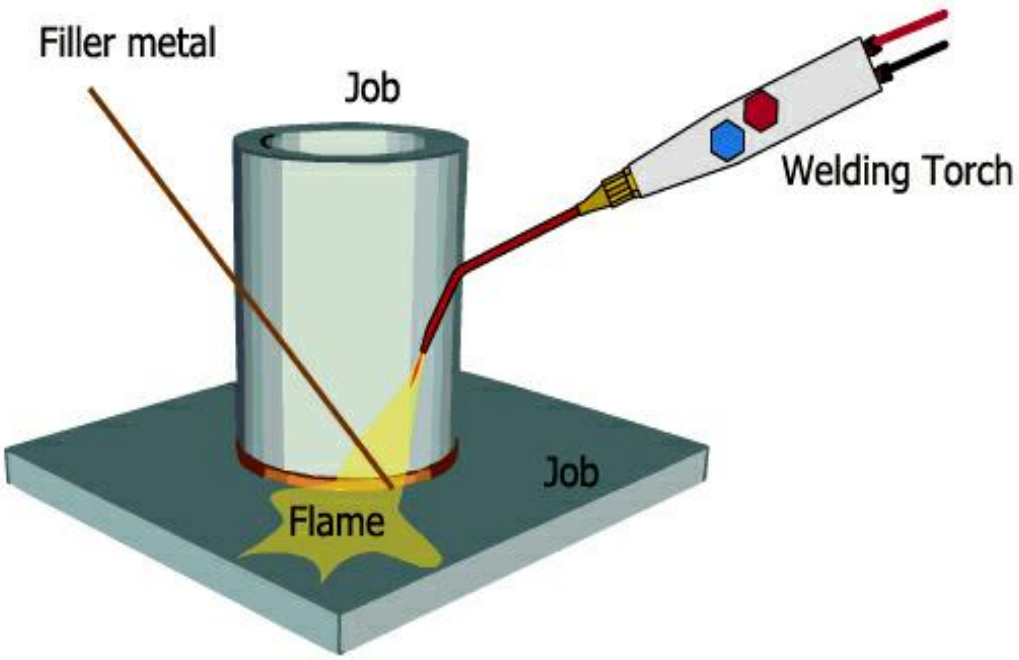

Figure 4. The brazing techniques process

1.1.6. Soldering

Soldering, similar to brazing is a joining process, which benefits from the capillary action of a melted metal filler with melting point (liquidus) of less than 450 °C, between the faying surfaces of the metal parts being joined [16]. As in brazing, the base metals are not melted, and the combination of the

separated base metals and creation of a metallurgical bond is achieved by melting the filler metal. Filler metal, called Solder, is added to the joint and is distributed between the closely fitting parts [16].

1.1.7. Explosion bonding

Explosion bonding is a solid-state process that is capable to directly join a wide variety of both similar and dissimilar combinations of metals that cannot be joined by any other approaches [17]. In solid state joining processes there is no need for a liquid interface (brazing) or the creation of a cast product by melting and re-solidification (welding). The combination between two separate pieces of materials through solid-state method is performed under the following conditions [18–20]:

(1) Applying the joining temperatures of below the melting point,

(2) Applying the joining load of less than the limits that would cause macroscopic distortion to the parts,

(3) Using a bonding aid such as an interface foil or coating to assist the joining process is sometimes recommended.

Moreover, joining the pieces with high surface areas has been possible through this method due to its potential to distribute the high energy density through explosion [17]. Although the explosive discharge engenders considerable heat, there is no sufficient time for heat transfer to the metal components; therefore, there is no substantial temperature increases in the metallic parts [17]. The quality and the mechanical strength of this joint is generally acceptable and high, and since it is a “cold method” the pre-bond properties of the bonded metals does not change during the process [17]. In this method, no melting occurs at the surface of the plates; instead, both surfaces plasticize and as a result a close contact between two surfaces is established which is sufficient to form a metallic bond [21, 22]. This principle is equivalent to other non-fusion welding techniques, such as diffusion bonding. In metals, the conduction

electrons are not bonded into a single atom, rather, they are free to move inside the metallic crystal lattice, behaving like a gas cloud and allowing the metal to conduct electricity [21, 22]. The positively charged ions, feel the electrostatic interaction of the conduction electrons, originating the metallic bond [21, 22].

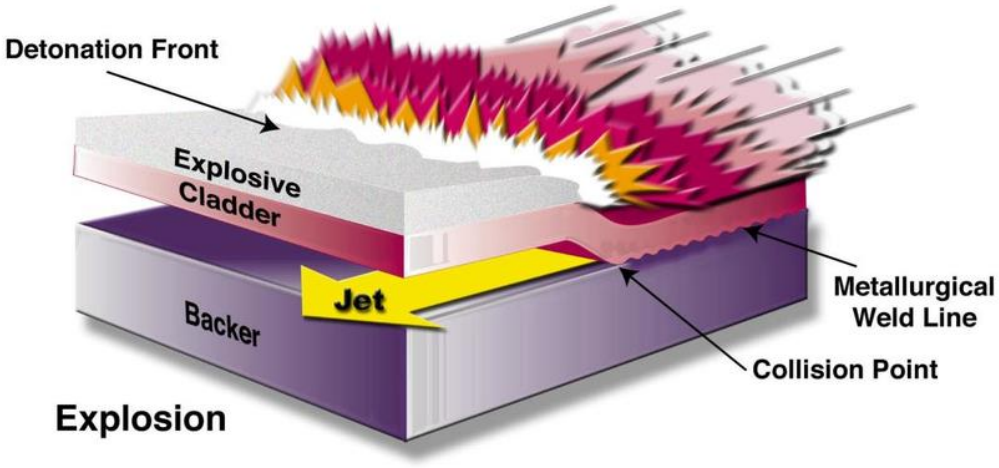

Figure 5. Schematic of the explosion bonding process [23]

During explosive welding processes, the shock drives the atom into the sphere of influence of each other's, forcing the conduction electrons into each other's paths [21, 22]. For this reason, the mechanical characteristics of an explosion bonded joint are theoretically not inferior to those of the base material. While the explosive welding process is successful, expensive failures occur and often the cause is unknown [21, 22].As schematized in Figure 5 the bonding is realized by placing explosive charges on top of one of the plates, the "cladder", and by controlling the detonation, which should occur progressively from one side to the other, in order to allow the jet formed between the cladder and the backer to come outside.

1.1.8. Diffusion bonding

Although this process was developed in the 1970s as a modern welding technology, the principle of the diffusion bonding process dates from former centuries when goldsmiths bonded gold over copper to create a product called filled gold. Initially, a thin layer of gold foil is produced and placed over copper, and a weight is placed on top of the foil. Finally, the assembly is placed in a furnace and left until a strong bond is obtained; hence, the process is also called hot-pressure welding (HPW) [24–26].

Diffusion binding as a solid state joining process, benefits from all advantages of the solid-state processes. Joining of materials by diffusion bonding can produce components without unexpected changes in microstructure and with a minimum of deformation [24–26]. In fact, diffusion bonding is a near net shaping process. By using this process, no supplementary machining or forming operation is required for the bonded components. Moreover, the structural inhomogeneity, which is caused through the temperature gradient, is minimized for diffusion bonded joints. Therefore, diffusion bonding is a cost-effective method that is able to produce components with minimum dimensional tolerances [27]. The diffusion bonded pieces interface is same as the base metals in physical and mechanical properties. The strength of a diffusion-bonded interface depends on the applied pressure and temperature of the bonding process, time of contact, and cleanliness of the faying surfaces [25–27].

Generally diffusion bonding is the most suitable approach for joining dissimilar metals. This process can be used for reactive metals such as titanium, beryllium, zirconium, and refractory metal alloys and for composite materials such as metal-matrix composites [24–26]. Diffusion bonding can be also used in powder metallurgy for sintering mechanism. The diffusion bonding process is slower than other welding processes because the diffusion occurs through the migration of the atoms across the joint [25,26,28]. Electronics/sensor industry, nuclear industry, aerospace and automotive industry use diffusion bonded engineering components in their products [25]. Besides metals and ceramics, diffusion bonding is also a

practical joining method that is used in heat-sensitive materials, materials with a tenacious oxide layer, and composites that are challenging to be combined by other processes [29].

1.1.8.1. Process of diffusion bonding

Diffusion bonding occurs through the inter-diffusion of atoms across the interface of the weld in the solid and, sometimes, the liquid state (when a molten interlayer is used) [25, 26,28,30]. The edges of the separated parts are moved within the range of atomic forces because of the applied bonding pressure (or pressing load). In terms of using a molten interlayer, the significant factor is the pressing load, which ejects the interlayer from the joint. Then pressing load is raised up until the interlayer is squeezed out of the joint [25, 26, 28, 30].

The diffusion bonding process will be ended by almost completely closing of the cavities at the contact surfaces by means of applied pressure and temperature to the interface for an arranged period of time [31]. The bonding temperature should be set between 50% and 70% of the melting point of the most fusible metal in the composition. The inter-diffusion of atoms across the interface of the weld is caused by the elevated temperature, which leads to surface deformation [26, 28]. The edges of the pieces should tightly contact together through the applied bonding pressure or pressing load [26, 28]. The applied load must be sufficient to deform the surface asperities and fill all the voids in the weld zone. Moreover, the pressing load disperses oxide films, which leads to improvement of the joint properties (e.g. strength) at the diffusion zone. Non-sufficient pressure may cause to existence of unfilled voids and reduce in joint strength. Another important parameter in the diffusion binding process is holding time [28]. According to the physical and economic considerations, there is a lower limit for the holding time (duration of pressure) at a definite bonding temperature and pressure [28]. Appropriate holding time would provide the sufficient time for formation of an appropriate contact and for accomplishment of the diffusion

processes [28]. An excessive diffusion time might result in presence of voids in the weld zone, change in chemical composition of the base metal, and formation of the brittle intermetallic phases (when dissimilar metals or alloys are being joined). The bonding environment is one of the effective parameters on the joint quality in this process [28]. Vacuum cleaning of the surfaces and removing the oxide films improve the material properties at the diffusion zone. Reducing atmosphere-using hydrogen can be considered as an alternative method for the cleaning of the surfaces. In some cases, an inert gas is used as a medium in the bonding process chamber [28].

The above-mentioned theoretical definition of the diffusion bonding process is generally applicable; however, the desired metal strength can be only achieved in case of materials that surface conditions do not obstruct atomic bonding; such as the absence of surface oxides or absorbed gases at the bonding interface [27, 28].

1.1.8.2. Mechanism of diffusion bonding

Depending on the materials that are involved in the diffusion process, numerous mechanisms of diffusion are available. Different mechanisms of diffusion can be mentioned as interstitial, collective, vacancy, and interstitial-substitutional exchange mechanism [26]. Although most of these mechanisms are related to solute atom diffusion, only a few number of these different diffusion mechanisms are applicable for pure metals. In terms of single-component metals, the diffusional flow of material is generally called the self-diffusion [32].

Mechanisms of diffusion in metals are closely related to the lattice point defects. The interstitial mechanism and the vacancy mechanism are two basic mechanisms of diffusion. In pure metals, the most probable mechanism of diffusion is the vacancy mechanism. However, the most probable mechanism of diffusion in case that impurities or solute atoms are involved in the diffusion process is the interstitial

mechanism [33]. In case of alloys, the diffusion mechanisms are more complex as compared to single-component metals. As mentioned before, the vacancy mechanism is the most common diffusion mechanism in pure metals, but the interstitial mechanism is also possible to occur in pure metals due to the self-interstitial atoms. Moreover, the interstitial mechanism can remove oxides and other impurities from metals that are required to maintain their original purity during the operations such as heat treatment [28, 34].

Diffusion bonding is a direct technological application of the diffusion phenomenon. The basic concept of the joining process in diffusion bonding is essentially the combination of two atomically clean solid surfaces. A three-stage metallurgical sequence of events is required to obtain a complete joining that can be seen in figure 6 at the first stage, the localized deformation of the contacting surface asperities grows the contact area to a large fraction of the joint area. Surface roughness, yield strength, work hardening, temperature, and pressure are of primary importance during the first stage of bonding. At the end of this stage, the planar shape of the interface boundary is changed, but the areas of intimate contact still consists of separated voids. In these areas of contact, the joint becomes equivalent to a grain boundary between the grains on each surface. The first stage usually ends in a short duration of time for the typical case of relatively high-pressure diffusion bonding. During the second stage of diffusion bonding, two changes occur simultaneously. The voids remained in the joints from the first stage shrink and most of them are eliminated.

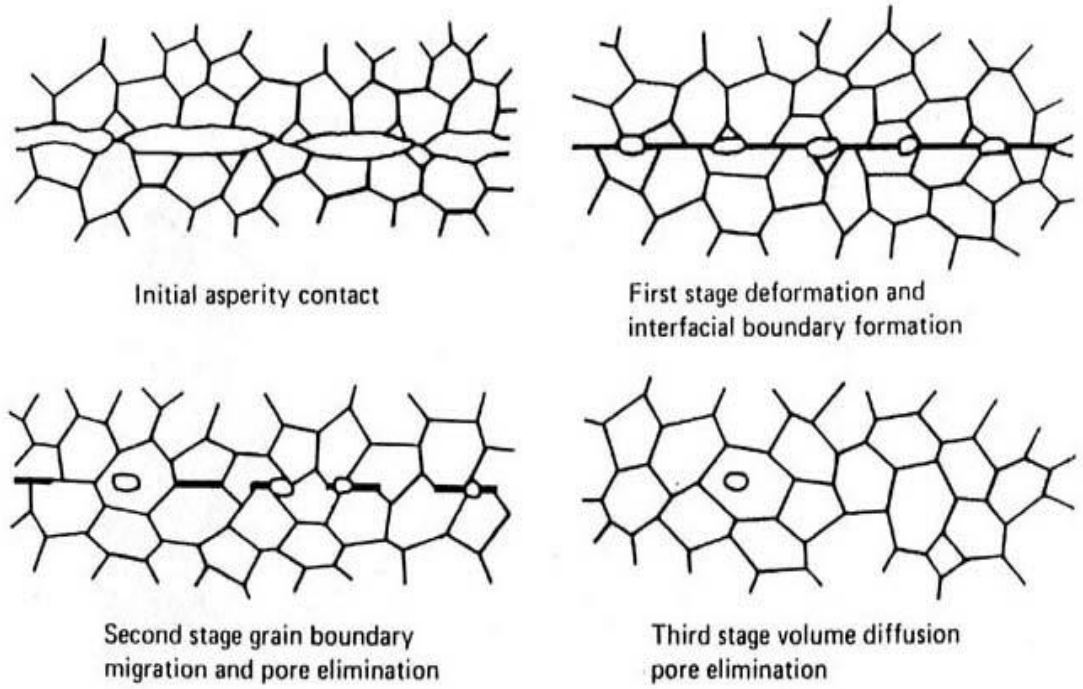

Figure 6. Schematic of the three stages of diffusion bonding [35]

In addition, the interfacial grain boundary migrates out of the plane of the joint to lower-energy equilibrium. The second stage of diffusion bonding fundamentally consists of creep and diffusion mechanisms. Most of the practical applications have shown that bonding would be considered essentially complete at the end of this stage. The remaining voids are surrounded by grains during the boundary moves, therefore they are no longer in contact with a grain boundary. As a result, during the third stage of bonding, the voids become very small and likely to not to effect on the interface strength. As the previous stage, in the third stage the shrinkage and elimination of voids occur through diffusional processes cause, but the only possible diffusion path in this stage is through the volume of the grains themselves [34].

1.1.8.3. Advantages and disadvantages of diffusion bonding

Same as other joining approaches, the diffusion bonding process has advantages and disadvantages, which should be addressed in order to choose the best production technology. The benefits of the diffusion bonding process are [24–26, 35]:

- Achieving high quality joints, without metallurgical discontinuities and porosity at the interface.
- Obtaining the strength and the ductility of the parent material by controlling the bonding parameters.
- Combination of different materials with different thermo-physical characteristics.
- Obtaining desirable dimensional tolerances.
- Welding possibility of complicate geometries or cross sections.
- Joining of the parts without pre-heating.
- Performing number of experiments simultaneously considering the dimensions of the machines (No limitations on the number of the joints).
- Independency of the bonding time from the bonded area.
- No need to expensive electrodes, solder or flux.
- Being cost-effective, apart the initial investment.
- No need to human/operation skill for the process since the process can be done using computer operating conditions.
- Being free from gas or ultraviolet radiation emissions.
- Maintaining health and safety standards.

The known limitations/disadvantageous of the diffusion bonding are as follows:

- Requiring great care in the surface preparation.
- High Initial investment.
- Unpractical technology for on-site applications due to the applied force and heat in vacuum or protective environments.
- Unsuitable for mass production, because of the long duration bonding time.
- Lack of reliable data about joint behavior (such as fatigue and fracture).

1.2. Dissimilar joint

It is worth mentioning that, in design process, the choice of appropriate materials is critical. For example, in the power generation industry, systems are supposed to operate at severe conditions of high temperature and pressure. Therefore, stainless steels are used to manufacture the components operating at high temperature systems while even ferritic steels are sufficient for those operating at lower temperatures. It is obvious that from the economic point of view the use of special materials, generally more expensive, should be limited to the zone (or the components) which bearing severe operating conditions. Consequently, dissimilar joints are unavoidable for linking the components/systems made of heterogeneous materials. For example, in steam generators, dissimilar metal combinations between pipes of ferritic steels and austenitic stainless steels are used. Besides the aforementioned methods, choose of dissimilar metals that can be joint together and also choose a capable method for joining them is the main objective [36]. Combination of dissimilar metals and alloys is a complex procedure due to the difference in the physical, mechanical and chemical properties of the components, which result in interactions between the metals and formation of the new phases [37]. The metals and alloys joining to each other may differ in melting point, density, temperature coefficient of linear expansion, lattice form, and lattice

constants. The refractory and chemically active metals such as titanium, niobium, tantalum and molybdenum, severely react with nitrogen and oxygen when heated (at a temperature of over 873 K), and this damages their properties [28].The dissimilar metal joints are likely to be disposed to the frequent failures [36] and these failures are generally due to the one or more of the following causes:

(a) Difference in mechanical properties through the weld joint and coefficients of thermal expansion (CTE) of the base metals and the consequential creep at the interface for example CTE for austenitic stainless steel and ferritic steel are generally 18 and 14×10-6/K, respectively [37,38].

(b) General alloying problems of the two different base metals such as brittle phase formation and dilution [39].

(c) Carbon migration from the ferritic steel into the stainless steel which weakens the HAZ region [37, 38, 40].

(d) Oxidation tendency at the interface [41, 42].

(e) Presence of residual stresses in the weld joints [42–44].

(f) Service conditions and other factors [45, 46].

1.2.1. Combination of Dissimilar materials

There are two combination methods of fusion and solid state welding to join dissimilar materials with entirely different physical and mechanical properties [47]. The joining approach is selected based on the type of dissimilar materials and the desired properties of the application [47]. Producing of dissimilar joints by fusion welding methods can supply the desired physical and mechanical properties. However, aforementioned joints in a corrosive environment, the secondary precipitates formed during fusion and

solidification critically corrodes and affects the integrity of the joints [47]. Solid-state processes are proposed for dissimilar joining of the materials with extremely different physical and mechanical properties [47].

1.2.1.1. Solid-state joining

Frequently solid-state joining procedures used to join dissimilar materials are pressure welding, roll bonding, explosion joining, friction welding, diffusion bonding and laser forming [47]. In solid state joining processes the hydrogen cracking and embrittlement of the joints are unlikely to happen in the service due to the absence of filler wires and electrodes [18, 20, 24]. Moreover, the formation of secondary precipitates is not probable because no melting occurs at the interface. Because of this, the corrosion resistance is not significantly affected during service. The most significant limitation of these procedures is that they are usually applicable for small components and therefore only selected important components are produced by these methods. The most appropriate dissimilar joining method for the desired application is chosen based on the joint properties, environmental considerations and process parameters. There are many parameters that affect the quality of the bond which is created between the two joining materials [25, 26, 28, 48, 49]. These parameters consist of surface preparation including good surface finish, freedom from contamination, wettability, scales and process layers, and the applied joining process. In a dissimilar joining procedure, two clean surfaces are brought together in close contact to produce strong adhesion over the force applied through several means. The presence of thin non-metallic layers and adsorbed gases on the bonding surfaces are two significant barriers to get a sound joint and to sustain a total matching surface over the total joining area. By applying pressure a bond can be produced; however, the lateral movement of the parts during the application of pressure can yield clean surfaces by asperity shearing [25, 26, 28, 48, 49].

1.2.1.2. Interlayer

The intermediate layers (interlayers) can be used to overcome the problems associated with the dissimilar joints that results in producing high-quality joints [30, 50]. Using interlayers in the diffusion bonding technology can greatly broadens the potentials and areas of application of this method. In many cases, interlayers are the only route to produce diffusion-bonded joints with appropriate physical and mechanical features in the combination of dissimilar materials [30]. The interlayer material is selected according to the properties of the base metals such as purity, surface roughness, and composition, the method of deposition, the thickness of interlayer, and the bonding conditions are also effective [30,50]. The advantages of using interlayers are mentioned as below [30,50]:

(a) Reducing the chemical heterogeneity and thermodynamic instability in the joined zone.

(b) Reducing and even preventing the thermal deformation effect on the base metals.

1.2.2. Examples of dissimilar (bimetallic) junctions

1.2.2.1. Copper-Copper joint

Copper materials are highly desirable as interconnectors due to the various reasons as mentioned below [1, 48,51–54]:

(a) Copper is a typical complementary Metal–Oxide–Semiconductor (CMOS) material.

(b) Copper forms reliable electrical bonds that provides conductive path between active layers in the stacked chip and provides strong strength.

(c) Copper has high electro migration resistance as conventional aluminum-based lines [54].

Although such bonds are often created under high operating temperatures (> 300°C), to achieve higher bond strength; a post-annealing process is also required under inert atmosphere [52,55]. Such severe conditions result in thermal-induced stresses within the chips that cause short time device reliability and high thermal budget. Direct copper–copper bonding are applying through thermo-compression bonding by application of heat and pressure simultaneously (typically about 350–400 °C and about 200 kPa) [41, 42]. Interdiffusion of copper atoms and grain growth are the principals of the bonding mechanism that is commonly known as diffusion bonding [1, 56]. The copper surface oxidizes that are formed in ambient air produce a barrier for successful diffusion bonding at low temperature. However, there is strong motivation to accomplish copper-copper bonding at low temperature results in better thermal budget control, lower thermal stress, and improved alignment [1, 56]. One method to bond at low temperatures is to clean and bond the copper surfaces in ultrahigh vacuum; however, this method is not appropriate from the manufacturing point of view [56]. The most successful method have been used so far is utilizing gas annealing or removal by wet cleaning to reduce oxides ;however, surface contamination of particles is still challenging [56,57]. The most influential parameters affecting the copper joint are bonding temperature, pressure, and time [25, 26]. In the presence of surface copper oxides in copper bonding, more thermal and mechanical energy is required to achieve a suitable joint [52]. This fact can clarify the reason why most of the successful copper-copper bonding processes are achieved in ultrahigh vacuum. Copper diffusion and grain growth are enhanced through the increase in pressure and temperature which brings about the better bond strength [52].

1.2.2.2. Stainless steel-Copper joint

Stainless steel plays a significant role in construction of modern accelerators and has wide range of grades. The most useful grades of stainless steel in construction and/or manufacturing technology are 316 LN, 316 L, and 314 L; in which, 316 LN is known as one of the most important one because it is widely used in manufacturing of magnet cold bore as a seamless tube [58]. In addition, this grade of stainless steel is the reference grade for the shrinking cylinder of the dipole magnets (2500 bent plates of 15.35 m of length, 10 mm thick for a total weight of approx. 3000 ton) [58]. A special Surface Tension Transfer (STT) technique combined with traditional pulsed metal inert gas (MIG) welding is used to weld the above mentioned plate. More than 2800 magnet end covers of complex shape including several nozzles, have been fabricated starting from HIPed 316 LN powders that have near net shaped into geometry close to the final form. Among magnets, 1600 interconnections consist of several thousands of leak tight components to be integrated, mainly working at cryogenic temperature (1.9 K). Austenitic stainless steels have a great role in fabrication of interconnection components [58]. The complexity of the several thousands of bellows involved in the machine and working under cyclic load at 1.9 K, made the researchers to introduce a special remelted 316 L grade of stainless steels which shows an extremely low inclusion content and also enhanced stability of the austenite at the working temperature [58,59]. It should be mentioned that remelted 316 L grade is highly formable at Room Temperature (RT) [59]. The most important grades of stainless steels for vacuum applications are 304 L, 316 L, and 316 LN [58]. The chemical composition of the abovementioned stainless steels based on Conseil Européen pour la Recherche Nucléaire (CERN) specifications is shown in Table 1.

Grade	C (wt.%)	Cr (wt.%)	Ni (wt.%)	Mo (wt.%)	Si (wt.%)	Mn (wt.%)	N (wt.%)	Others (wt.%)
304 L	0.03	17.00-20.00	10.00-12.50		1.00	2.00		P≤0.045, S≤0.030 Co≤0.2
316 L	0.03	16.00-18.50	11.00-14.00	2.00-2.50	1.00	2.00	0.05	P≤0.030, S≤0.010 Co≤0.2
316 LN	0.03	16.00-18.50	12.00-14.00	2.00-3.00	1.00	2.00	0.14-0.20	P≤0.045, S≤0.015 Co≤0.2

Table 1: The chemical compositions of 304 L, 316 L, and 316 LN grades of stainless steel

304 L grade has general applications in heat exchangers, automotive and aerospace structures, and buildings. In order to use this grade in vacuum applications, it should be treated through a several special operations, to obtain a substantially austenitic microstructure and to control the level of inclusions [58]. There are limited concentrations of alloying elements in this grade of stainless steel hence martensitic transformation can enhance the magnetic susceptibility of 304 L grade. The martensitic transformation is achieved upon cooling the component to room temperature or to cryogenic temperatures. The following work hardening operations are performed at room temperature or less than room temperature [60]. 316 L is a molybdenum containing grade; in which, molybdenum improves austenitic stability and corrosion resistance through the martensitic transformation stage. To achieve an almost fully austenitic microstructure the ferrite-promoting characteristics of molybdenum should be adjusted by using chromium and nickel as alloying elements. 316 L grade have greater formability, ductility and austenitic

stability compared to 304 L grade. Due to the above-mentioned properties a special CERN specification covered this grade to reduce difficulties of the LHC interconnections [58]. 316 LN is a nitrogen containing stainless steel; in which, nitrogen enhances austenite stability through martensitic transformations and is a strong austenite former. Nitrogen in chemical composition of the stainless steel can substantially increase strength along with maintaining ductility down to cryogenic temperatures [61]. Stainless steel and copper combination have many industrial applications due to the beneficial properties of the bimetal. This type of combination has an increasing demand in automobile, rail and aviation industry. Vessel fragments of international thermonuclear experimental reactor are joined through combination of stainless steel and copper in power generation plants [48]. Based on successful applications of austenitic stainless steel in the nuclear environments of light water and faster breeder reactors, this joint is selected as a primary structural material for first wall/blanket system. Furthermore, copper is the most applicable metal in heat fluxes of diverter because of the good conductivity and thermal stress resistance [53]. Although the combination of stainless steel and copper alloys is of great importance in industrial productions, achievement of this joint become a challenging task due to their obvious mismatches, such as thermomechanical properties, physical properties and chemical properties [48]. Previously, arc welding procedures such as gas tungsten arc welding, gas metal arc welding, and submerged arc welding is used for joining stainless steel and copper. Despite the widespread use of this method, it was incapable of providing a defect-free dissimilar stainless steel and copper alloy joint [62]. To overcome aforementioned problem and to improve the microstructure and properties of stainless steel/copper joints, electron-beam welding, laser welding, friction welding, explosive welding, and diffusion bonding we used [48]. Among these methods, diffusion bonding is considered as an appropriate method that can minimize deleterious effects such as crack, distortion and segregation on material properties [48].

1.3. Design of experiment (DOE)

Design of experiments (DOE) is a planned approach for determining cause and effect relationships [63]. Any process with measurable (both qualitative and quantitative) inputs and outputs can be investigated by this method. Indeed, DOE is a strong approach for exploring new processes, gaining a deeper knowledge of the processes and optimization of the processes [63]. DOE is useful for two essential experimental stages of screening and optimization regardless of place that the experimental investigation were conducted (laboratory, the pilot plant, or the full-scale production plant). In a designed experiment, the engineer often makes deliberate changes in the input variables (or factors/parameters) and then investigates the trend that the output variable (response) varies consequently. Obviously, each variable affect the response on its own way (strong, medium, or no effect). Therefore, the results of the designed experiments are investigated to determine which set of input variables in a process affects the responses most and then define the best range or levels for these variables to obtain the optimum parameters for achieving the desirable responses [64]. The essential advantage of using DOE is that it provides a systematically approach to solve both simple and complex experimental problems. After selecting an appropriate experimental objective to investigate, the supposed effective design parameters can be chosen. Then, DOE guides the experimenter to design and perform a set of experiments, which is adequate for the selected objective. It should be noted that a sets of responses could be considered in DOE design, which means that multiple response can be optimized at the same time. The experiments designing by DOE require fewer experiments to investigate and optimize the procedure than any other approach [63]. In addition, these limited experiments are mutually connected and thereby linked in a logical and theoretically favorable manner because they belong to an experimental plan. In addition, it is able to evaluate the interactions and influence of all factors, which make it useful and reliable approach for conducting experiments and interpreting the obtained information. In order to minimize the

experimental error, experiments are performed in random order. Using randomization, the effects of noise factors that may be present in the process are dispersed between the experiments and are minimized. In other words, randomization can balance the noise factors through all levels of designed factors. Replication is the other benefit of DOE that has two important advantages; in which, the first one is estimation of the experimental error and the latter one is accurate estimation of the factor/interaction effects [63]. As mentioned before, DOE is useful for two essential experimental stages of screening and optimization, which are explained in the following sections.

1.3.1. Screening

Usually there are many potential design parameters (factors) and levels in many process development and manufacturing applications. Screening can determine the chief factors and levels that affect product quality or process performance and decrease the number of design parameters. This reduction provides the opportunity to allocate the cost and time to investigate the few important factors or the vital few. Screening is used at the beginning of the experimental procedure. The objective of the screening can be shortened in the two following reasons:

(a) Determining the influential operating parameters on the response.

(b) Defining the appropriate ranges/levels of the effective design parameters.

1.3.2. Optimization

After investigating, the most influential parameters and levels optimization experiments can be conducted. The objective of the optimization stage can be mentioned as below:

(a) Predicting the response model for all possible values of the design parameters within the experimental ranges.

(b) Determining the optimum experimental conditions.

Contrary to the screening, optimization designs require many experiments in relation to the number of investigated factors.

1.3.3. Approach overview

In this study, the diffusion bonding process of stainless steel of grade 316 L and pure copper (99.99 wt. %) is investigated. The solid state diffusion bonding process has the advantages of lower temperature, minimum microstructure change and deformation, more cost efficiency, lower porosity in the joined area, higher join strength and, etc. in comparison to the other solid and liquid state joining methods [25, 26, 48]. The effects of four parameters of type of interlayer, bonding pressure, bonding temperature, and holding time are investigated on the tensile strength and shear strength of the bonded joints. The experiments were designed at two stages of screening and optimization by Design Expert 7 (State-Ease Inc., Minneapolis, MN, USA) software. At first, 16 Experiments based on factorial design were carried out as screening tests to find the most influential parameters and levels. The diffusion bonding process was then optimized using central composite design (CCD) by the goal of achieving the maximum tensile and shear strength in the performed range of the parameters. Eventually the proposed optimized condition was confirmed using three confirmation experiments. The microstructure of the bonded joints were examined by high-resolution scanning electron microscopy (HR-SEM) and energy dispersive X-ray spectroscopy (EDS).

1.4. Related studies (literature review)

In a study which was performed by Negemiya et al. [65], diffusion bonding was accomplished between Ti–6Al–4V alloy and AISI 304 austenitic stainless steel utilizing copper as an interlayer in the holding time variety of 45–105 min for 925 °C under 14 MPa load in a vacuum. After bonding, the microstructural study including metallographic examination and energy dispersive spectroscopy, micro hardness survey, shear strength test, and tensile test were accomplished. From the results, holding time was reported to be a major influence to develop the microstructural characteristics and improve the joints quality. The various intermetallic compounds of CuTi, Cu_3Ti_2, FeTi, Fe_2Ti, Cr_2Ti has been reported to be formed based on the ternary phase diagrams of Fe–Cu–Ti and Fe–Cr–Ti. The highest bond strength of 268 MPa was attained for the pair bonded at 90 min holding time. With the expansion during the higher holding time up to 105 min, the quality was reduced caused by the expanded volume fraction of discontinuities. Meng et al. [66] fabricated a composite plate of low carbon steel and pure zirconium by diffusion bonding with Cu-base amorphous interlayer at a temperature of 700 °C and pressure of 3 MPa. The effect of interlayer thickness on the microstructure and properties of the composite plate were investigated. The results show that all the samples produced with various interlayer thicknesses are composed of the reaction layer (RL) with a multilayer structure. Two dendritic structures are observed in the RL with 90 μm thick interlayer. It was reported that the maximum shear strength across the composite plate and the displacement is 88 MPa and 0.33 mm, respectively. The maximum bending strength and strain of the composite plate reached 1079 MPa and 47.6%, respectively. In the study conducted by Zhang et al. [1] a direct diffusion bonding method was designed to bond tungsten (W) and copper (Cu) without using an interlayer metal at a temperature close to the melting point of copper (T_{mCu}). The results showed that the direct diffusion bonding method was feasible and the key point to a successful connection is that bonding temperatures should be controlled in an effective temperature range 0.81 T_{mCu}–0.97 T_{mCu}. The most

appropriate bonding parameters were the bonding temperature of 980 °C, the bonding time of 180 min and the bonding pressure of 106 MPa. The maximum tensile and bending strengths of the as-obtained W/Cu joints were ca. 172 and ca. 232 MPa, respectively, which reached a very high level compared to pure copper. The corresponding fractures were ductile. The micro-tests for the W/Cu joint show that diffusion occurs between W and Cu and the thickness of the W/Cu diffusion layer was ca. 22 nm. Through the diffusion, a metallurgical bonding interface was successfully constructed, which was the essential reason for the high strengths of the W/Cu joint. They suggested that the diffusion between W and Cu when the bonding temperature was close to T_{mCu} might have been induced by the high-temperature structure of Cu. Srikantha et al. [67] developed a methodology based on diffusion bonding for joining stainless steel (SS) type 304L and Zircaloy-4 using Ni and Ti interlayers. Diffusion bonding was performed in the range of 800 °C–900 °C under vacuum for different time intervals varying between 30 and 90 min. The bonding parameters were optimized at bonding temperature of 850 °C for 60 min duration, when the maximum shear strength of 209 MPa was obtained. The SS 304L/Zircaloy-4 joint interfaces showed the formation of different intermetallics like NiZr2, NiZr, Ni3Ti, NiTi and NiTiZr in layered morphology. The interface of the joint bonded at 900 °C showed the formation of Ni-Zr type intermetallics, while those of the joints bonded at 800 °C and 850 °C showed the presence of Ni-Ti type intermetallics. The phases present on the both SS and Zircaloy fracture surfaces were identified as NiTiZr for bonding conditions of 850 °C and 60 min and as NiZr2 for the bonding conditions of 900 °C and 30 min. In another study, Singh et al. [68] employed a diffusion bonding technique for the joining of WCu-CuCrZr material with nickel interlayer and titanium interlayer by using a Gleeble 3800 system. Diffusion bonding experiments were performed at various temperatures (600 °C, 650 °C, 700 °C, 750 °C, 800 °C, 850 °C & 900 °C) with the uniaxial pressures of 5 MPa, 10 MPa and 15 MPa and a constant dwell time of 15 min. The bonded specimens were characterized using non-destructive testing (ultrasonic

examination of diffused region) and destructive testing (shear testing and micro hardness examination). The effect of the test parameters on the bonding strength has been studied and evaluated with respect to various inter-layers. The diffusion bonded joint was qualified for 1000 cycles at 450 °C. The diffusion bonding capability between $Zr_{41.25}Ti_{13.75}Cu_{12.5}Ni_{10}Be_{22.5}$ bulk metallic glass and pure Cu with and without interlayer was studied on a Gleeble3500 thermomechanical simulator by Hongchao et al. [69]. They reported that the diffusion bonding joints between $Zr_{41.25}Ti_{13.75}Cu_{12.5}$-$Ni_{10}Be_{22.5}$ BMG and copper can be formed at the super-cooled liquid region temperatures based on the superplastic property of Zr-based BMG. Experimental results showed that good diffusion bonding joints without cracks and voids can be obtained under both conditions—with and without Ni foil. Atomic diffusion at the interface was obviously observed by using EDS and EPMA methods, while the diffusion zones were very narrow. The crystalline phases transformed from amorphous state accelerated the atomic diffusion at the interface. Crystalline phases detected when the bonding temperature reaches 683 K, which accelerates the atomic diffusion at the interface. The joining of SS 316 L material to CuCrZr material was investigated in the study which was performed by Singh et al. [70]. In this study, the diffusion bonding technique was adopted as a process for joining of these two dissimilar materials. Thermo-mechanical simulator machine (Gleeble 3800) was used to perform diffusion bonding experiments at different temperatures—650◦C, 850◦C, 900◦C, 950◦C & 1000◦C—different uniaxial pressure varying from 5 MPa to 15 MPa and with the holding time of 15 min & 30 min, by using pure nickel interlayer. The diffusion bonded samples have undergone non-destructive testing (NDT) particularly the ultrasonic examination using immersion probe technique, microstructural examination by the High Resolution (HR) electron microscopy (SEM), Energy Dispersive X-ray (EDAX) analysis, micro hardness measurement and shear measurements by custom made fixture. The diffusion bonding parameter of SS 316 L/CuCrZr was optimized based on this study—with Nickel (Ni) interlayer and without interlayer. Pardal et al. [71] used the low thermal heat

input process cold metal transfer (CMT), when compared with conventional GMAW, to deposit a copper (Cu) bead between Ti and stainless steel. Cu is compatible with Fe, and it has a lower melting point than the two base materials. The welds were produced between AMS 4911L (Ti-6Al-4V) and AISI 316 L stainless steel by using a CuSi-3 welding wire. The joints produced revealed two IM layers located near the parent metals/weld interfaces. The hardness of these layers was higher than the remainder of the weld bead. Tensile tests were carried out with a maximum strength of 200 MPa, but the interfacial failure could not be avoided. Ti atomic migration was observed during experimental trials; however, the IMC formed are less brittle than FeTi, inducing higher mechanical properties. The binary phase Ti-6Al-4V alloy was joined with duplex stainless steel (DSS) by the diffusion bonding process in a lower temperature range of 650–800◦C in a study which was conducted by Velmurugan et al. [72]. An axial load of 10 MPa was applied for 30 min to create the joint under vacuum state. Microstructural Characterization of the bonded interface was analyzed using optical and scanning electron microscopy. The composition of elements presented near the bonded interface was measured using Energy Dispersive Spectroscopy (EDS). The interlayer growth kinetics and activation energy were evaluated using Arrhenius relationship. The diffusion coefficient of the interface elements under different temperatures were determined by Fick's law. The quality of the bond was assessed by the mechanical shear test and micro hardness. The fractured surfaces were analyzed and fractographs were prepared using XRD for the joint, bonded at 750◦C which had more shear strength by hard intermetallic of Fe-Cr-Ti. Wang et al. [73] proposed a pulse electro-deposited Fe-W amorphous alloy forming on a copper sheet as an interlayer to join W and Cu via vacuum diffusion bonding. It was found that an improvement in bonding strength and a decrease in bonding residual stresses was obtained by the bidirectional diffusion of Fe in the form of highly active amorphous state in W and Cu at the weld temperature. The diffusion transition regions were formed near the W/Cu interface which consists of a solid solution zone and various phases between the

Fe-W and Fe-Cu binary systems and two different fracture phenomena were observed on the basis of the microstructural characteristics. With the introduction of this new kind amorphous coating as an interlayer, the vacuum diffusion bonding joint of W and Cu heating at 950°C for an hour with a load of 30 MPa showed a maximum tensile strength of about 146 MPa. In another investigation [74], the liquid state diffusion bonding mechanism of stainless steel 316 to Ti-6Al-4 V by using pure Cu interlayer has been investigated at 1100°C for 60 min bonding time. The microstructure of joint zone was analyzed in detail by scanning electron microscope and energy dispersive spectroscopy. The micro hardness and shear strength tests were also applied to characterize mechanical properties of the joints. The results showed that increasing the interlayer thickness led to the extension of diffusion zone and the increase of final joint width. The maximum shear strength of 284 MPa was obtained for the bond made with 50 mm thick interlayer while with an increase in interlayer thickness, the shear strength values decreased to 145 MPa that could be attributed to formation of brittle intermetallics such as Cu_2Ti and CuTi at the interface. To minimize the residual stress induced by the large mismatch of thermal expansion coefficients and to inhibit the formation of brittle intermetallic phases, a V/Cu composite barrier interlayer was designed and examined to produce a joint between W and steel by Cai et al. [75]. The diffusion bonding was carried out at 1050 °C for 1 h under a 10 MPa pressure in vacuum. Metallographic analysis revealed excellent bonding at all of the joining interfaces. Neither intermetallic compounds nor other brittle phases were found in the bonded region. Nano-indentation test across the joint interfaces demonstrated the effect of solid solution strengthening in the diffusion zone. The strength of the joint was reported to be as high as 402 MPa and the failure occurred predominantly at the W substrate near the W/V interface due to the residual stress concentration. In the study of Yuan et al. [48] impulse pressuring diffusion bonding of a copper alloy to a stainless steel was performed in vacuum. Using Ni interlayer of 12.5 lm, the joint produced at 825 °C under 5–20 MPa for 20 min exhibited lower strength, which could result from the

insufficient thermal excitation and plastic deformation. At 850 °C under 5–20 MPa for 5–20 min, the strength of the joint improved with time. An optimized joint strength reached up to 217.2 MPa. Fracture occurred along the Cu–Ni reaction layer and the Ni layer and almost plastic fracture was confirmed by extensive dimples on the fracture surface. Using the interlayer of 50 lm, the fracture surface was similar. Without Ni assistance, under the same bonding condition, the joint strength was about 174.2 MPa. They suggested that the lowered strength might have been attributed to the appearance of some unbonded zones in the joint due to the reason that lots of brittle fracture areas appeared on the fracture surface. In another study, Szwed and Konieczny [76] joined titanium and X5CrNi18-10 stainless steel samples by diffusion bonding using copper foil as a filler metal at temperatures of 850, 875, 900, 925, 950 and 1000 °C. The structural examinations have shown significant changes in joints and relatively expansive diffusion zones on the borders of the joined materials. Structures of joints depended on the temperature of the process. The structure of the joint from the titanium site was composed of the eutectoid mixture $\alpha Ti+CuTi_2$ and layers of phases $CuTi_2$, CuTi, and Cu_4Ti_3. From the stainless steel site of joint in all samples, regardless of the temperature of the process, there were formed layers of FeTi phase, and additionally layers of Fe_2Ti at 925, 950 and 1000 °C. The maximum shear strength was reported to be achieved for joints performed at 900 °C. In the study of Aydin et al. [77], Ti–6Al–4V alloy was bonded to electrolytic copper at various temperatures of 875, 890 and 900 °C and times of 15, 30 and 60 min through diffusion bonding. 3 MPa uniaxial load was applied during the diffusion bonding. Interface quality of the joints was assessed by micro hardness and shear testing. Also, the bonding interfaces were analyzed by means of optical microscopy, scanning electron microscopy and energy dispersive spectrometer. The bonding of Ti–6Al–4V to Cu was successfully achieved by diffusion bonding method. The maximum shear strength was found to be 2171 N for the specimen bonded at 890 °C for 60 min. The maximum hardness values were obtained from the area next to the interface in titanium side of the

joint. The hardness values were found to decrease with increasing distance from the interface in titanium side while it remained constant in copper side. It was seen that the diffusion transition zone near the interface consisted of various phases of bCu4Ti, Cu2Ti, Cu3Ti2, Cu4Ti3, and CuTi. Lee et al. conducted [78] an study to find the optimum condition for diffusion bonding of copper and steel. The experimental were performed at 3 different pressures and temperatures range from 800°C to 950°C. In order to characterize the flow strength of materials at high temperatures, several tensile tests were performed at several temperatures from 800°C to 950°C. Mechanical properties of the bonded specimen were evaluated through tensile and shear tests. Microstructure of bonded layer has been also observed with SEM with EDX. The results showed that the optimum condition of diffusion bonding was 7 MPa, 890°C, and one hour contact time. In an investigation that was performed by Sabetghadam et al. [79] plates of stainless steel (grade 410) were joined to copper ones through a diffusion bonding process using a nickel interlayer at a temperature range of 800–950 °C. The bonding was performed through pressing the specimens under a 12-MPa compression load and a vacuum of 10−4 torr for 60 min. The results indicated the formation of distinct diffusion zones at both Cu/Ni and Ni/SS interfaces during the diffusion bonding process. The thickness of the reaction layer in both interfaces was increased by raising the processing temperature. The phase constitutions and their related microstructure at the Cu/Ni and Ni/SS diffusion bonding interfaces were studied using optical microscopy, scanning electron microscopy, X-ray diffraction and elemental analyses through energy dispersive spectrometry. The resulted penetration profiles were examined using a calibrated electron probe micro-analyzer. The diffusion transition regions near the Cu/Ni and Ni/SS interfaces consist of a complete solid solution zone and of various phases based on (Fe, Ni), (Fe, Cr, Ni) and (Fe, Cr) chemical systems, respectively. The diffusion-bonded joint processed at 900 °C showed the maximum shear strength of about 145 MPa. The maximum hardness was obtained at the SS–Ni interface with a value of about 432 HV. Elrefaey et al. [24] joined dissimilar

titanium/steel metals by diffusion bonding process with the help of a copper-based interlayer. The appropriate processing parameters have been investigated and the joints were analyzed by means of scanning electron microscopy (SEM), micro hardness measurement, shear strength test, and X-ray diffraction (XRD). The results show that the joint could not be bonded at a temperature lower than 800 ◦C even at holding time of 180 min. However, at 850 ◦C successful joining was achieved at all holding times. On the other hand, atom diffusion and migration between Ti and Fe or C were effectively prevented by adding a copper-based interlayer and hence, Fe–Ti and Ti–C intermetallics were not formed in the joint. They implied that this technique provides a reliable method of bonding titanium to steel. In the investigation performed by Xiong et al. [80], vacuum diffusion bonding of stainless steel to copper was carried out at a temperature ranging from 830 to 950 °C under an axial pressure of 3 MPa for 60 min with three kinds of interlayer metals: tin-bronze (TB) foil, Au foil, and TB-Au composite interlayer. The results showed that the grain boundary wetting was formed within the steel adjacent to the interface due to the contact melting between TB and Au in the case TB-Au composite interlayer had been used. The tensile strength of the joint with TB-Au was higher than that with TB or Au interlayer separately and could be 228 MPa at the joining temperature of 850 °C. Furthermore, the axial compression ratio of the specimen joined at 850 °C was approximately 1.2%. Accordingly, they reported a reliable and precise joining of stainless steel to copper was achieved through diffusion bonding with the TB-Au composite interlayer at a comparatively low temperature. Mahendran et al. [81] joined Mg–Cu dissimilar materials by diffusion bonding process. Because The principal difficulty when joining Mg–Cu lies in the existence of hard-to-remove oxide films on the magnesium surfaces and the formation of brittle metallic interlayers and oxide inclusions in the bond region, in this investigation, an attempt was made to develop diffusion bonding windows for effective joining of AZ31B Magnesium and commercial grade copper alloys. Joints were fabricated using different combination of process parameters such as bonding temperature, bonding

pressure and holding time. The bonding quality was checked by microstructure analysis and lap shear tensile test. Based on the results, diffusion bonding windows were constructed, and they are presented in this paper. They implied that these windows act as reference maps for selecting appropriate diffusion bonding process parameters to get good quality bonds for Mg–Cu alloys. In a study which was performed by Kundu et al. [82] diffusion bonding was carried out between commercially pure titanium (cpTi) and 304 stainless steel (304ss) using copper as interlayer in the temperature range of 850–950 ◦C for 1.5 h under 3MPa load in vacuum. The microstructures of the transition joints were revealed in optical and scanning electron microscopy (SEM). The study exhibited the presence of different reaction layers in the diffusion zone and their chemical compositions were determined by energy dispersive spectroscopy. The occurrence of different intermetallic compounds such as $CuTi_2$, CuTi, Cu_3Ti_2, Cu_4 Ti_3, FeTi, Fe_2Ti, and Cr_2Ti was reported based on the ternary phase diagrams of Fe–Cu–Ti and Fe–Cr–Ti. These reaction products were confirmed by X-ray diffraction technique. The maximum bond strength of ∼318MPa (∼99.7% of Ti) was obtained for the couple bonded at 900 ◦C due to better coalescence of mating surface. With the rise in joining temperature to 950 ◦C, decrease in bond strength occurs due to formation of brittle Fe–Ti bases intermetallics. At a lower joining temperature of 850 ◦C, bond strength was also lower due to incomplete coalescence of the mating surfaces. Eroglu et al. [83] used diffusion bonding to join Ti–6Al–4V alloy to a micro duplex stainless steel using a pure copper interlayer. The effects of heating rate and holding time on microstructural developments across the joint region were investigated. After bonding, microstructural analysis including metallographic examination and energy dispersive spectroscopy (EDS), micro hardness measurements, and shear strength tests were carried out. From the results, it was seen that heating rate and holding time directly affect microstructural development at the joint, especially with respect to the formation of TiFe intermetallic compounds, and this in turn affects the shear strength of the bonds. A sound bond was obtained with a heating rate of 100 K min^{-1} and holding

time of 5 min, and this was related to the small amount of TiFe intermetallics formed close to the duplex stainless steel side at this bonding condition. Although Ti_2Cu and TiFe intermetallics were formed in all specimens, it was seen that the most deleterious intermetallic was TiFe. As the heating rate was decreased and holding time increased the amount of TiFe intermetallics increased, and consequently shear strength decreased. As a result, from the microstructural observations, EDS analysis, micro hardness measurements, and shear strength tests, it was concluded that a high heating rate and a short holding time must be used in the diffusion bonding of Ti–6Al–4V to a micro duplex stainless steel when pure copper interlayers are used. Nishi et al. [84] investigated the diffusion bonding of alumina dispersion-strengthened copper (DS Cu) to 316 stainless steel which was carried out with interlayer metals such as Au, Cu and Ni foil in order to investigate the influence of the interlayer metals and bonding conditions on strength of the joints. The tensile strength of joints with an Au interlayer was superior to those with Cu and Ni interlayer metals and similar to that of DS Cu base metal. The tensile strength of joints with a Cu and Ni interlayer was less than that of immediate diffusion bonding joint for the DS Cu to 316 stainless steel. The Charpy-absorbed energy of the Au interlayer joint increased up to 50% of DS Cu, while that of the immediate diffusion bonding joint was only 20%. Concerning the microstructure of the Au interlayer joints, intermetallic compounds consisting of B, Fe and Cr were observed in the Au interlayer. For the Ni interlayer joints, Kirkendall voids were formed in the DS Cu near the interface where the specimen fractured. The specimens with the Cu interlayer fractured at the interface between DS Cu and Cu interlayer. They suggested that the degradation of the strength of the joints with the Cu interlayer is attributed to the diffusion rate between the Cu interlayer and the DS Cu. Based on the extensive and critical applications of copper-stainless steel 316 joints in industry and in order to improve the findings of the previous researches—mentioned before—the present thesis in about to investigate the diffusion bonding of stainless steel of grade 316 L and pure copper (99.99 wt.%).

2. Experimental

2.1. Materials and preparation

In this study, stainless steel of grade 316 L and pure copper (99.99 wt.%) in the form of coupons with dimension of 100×50×10 mm were used as the base metals for the solid state diffusion bonding process. Nickel foil of 20-μm thickness and 99.99 % purity were used as the interlayer metal. Silicon carbide (SiC) paper to a 2000-grit was used to grind the surface of the coupons; then specimens were finished and polished manually. In order to remove the damages of the cutting operation and provide a flat surface. The metal specimens were degreased with acetone in an ultrasonic bath for 60 min to remove adhered contaminations prior to the diffusion bonding process. Both surface sides of the interlayer foils were ground and degreased using aforementioned route.

2.2. Design of diffusion bonding experiments

There are different methods for designing experiments like one factor at a time; i.e., changing a parameter gradually while all other parameters are being kept fixed. This method is unable to determine the interactions between the operating parameters and, therefore, the optimum condition cannot be estimated. Therefore, to achieve numerical equations between the input factors and calculate statistical model of the factors effect on the responses, the effects of operating parameters in the process of diffusion bonding of stainless steel of grade 316 L and pure copper (99.99 wt.%) was studied using DOE method by means of Design Expert 7 software (State-Ease Inc., Minneapolis, MN, USA). In order to reduce the number of experiments and determine the most influential parameters, the experiments were conducted in two stages of screening and optimization. At first four possible effective parameters of bonding pressure (5 and 15 MPa), bonding temperature (800 and 1000 °C), holding time (30 and 60 min), and interlayer (with nickel and without nickel) from literatures were determined for screening stage. Table 2 shows the 16

experiments were designed in screening stage using factorial method to identify influential parameters and levels.

Standard order	Parameters				Responses (MPa)	
	Interlayer	Pressure (MPa)	Temperature (°C)	Holding time (min)	Tensile strength	Shear strength
1	Nickel	5	800	30	240	57
2	None	5	800	30	225	50
3	Nickel	15	800	30	247	60
4	None	15	800	30	239	53
5	Nickel	5	1000	30	332	87
6	None	5	1000	30	310	75
7	Nickel	15	1000	30	400	90
8	None	15	1000	30	353	78
9	Nickel	5	800	60	243	58
10	None	5	800	60	228	52
11	Nickel	15	800	60	249	61
12	None	15	800	60	239	54
13	Nickel	5	1000	60	333	85
14	None	5	1000	60	309	76
15	Nickel	15	1000	60	405	93
16	None	15	1000	600	357	79

Table 2. The screening experiments based on factorial design

Afterwards, at the optimization stage, the most influential parameters and levels obtained from the screening experiments were used in a response surface methodology (RSM)-central composite design (CCD) to determine the optimum condition of the diffusion bonding process. Table 3 shows the optimization experiments and the obtained results which will be discussed in the result section.

Standard order	Parameters		Responses (MPa)	
	A: Pressure (MPa)	B: Temperature (ºC)	Tensile strength	Shear strength
1	5.00	800.00	240.00	57.00
2	15.00	800.00	247.00	44.00
3	5.00	1000.00	332.00	87.00
4	15.00	1000.00	400.00	90.00
5	2.93	900.00	240.00	36.00
6	17.07	900.00	433.00	118.00
7	10.00	758.58	227.00	38.00
8	10.00	1041.42	330.00	88.00
9	10.00	900.00	432.00	101.00
10	10.00	900.00	430.00	100.00
11	10.00	900.00	429.00	102.00
12	10.00	900.00	430.00	101.00
13	10.00	900.00	428.00	99.00

Table 3. The optimization experiments

CCD is the most successful and best factorial design which is accomplished by adding two experimental points along each coordinate axis at opposite sides of the origin and at a distance equal to the semi-diagonal of the hyper cube of the factorial design and new extreme values (low and high) for each factor added in this design [63]. Based on the screening step temperature and pressure in two levels of 800 and 1000 °C as well as 5 and 15 MPa were identified as the most influential parameters as compared to holding time and interlayer. The goal is to find a desirable location in the design space to enhance the diffusion bonding process of stainless steel of grade 316 L and pure copper (99.99 wt.%) by optimizing the operation parameters where the response is stable over a range of the parameter. The experiments were performed in a random order to eliminate the effect of systematic errors to the extent possible.

2.3. Diffusion bonding experiments

Currently, CECOM neither have technology nor the required knowledge for diffusion bonding. Therefore, the diffusion bonding experiments were performed as an external phase, provided by PVA TePla AG, Wettenberg, Germany. The company, represented by Christian Eckardt, collaborated with CECOM for qualifying the process. PVA TePla AG is employing resistance heated high vacuum heat treatment furnace with integrated pressing unit to perform diffusion bonding. In this technology, the samples are fixed by means of a pressing force in the vacuum environment and heated and pressed homogenously until the diffusion occurs and the separated pieces are joined. Figure 7 shows the diffusion bonding resistance heated high vacuum heat treatment furnace with integrated pressing unit.

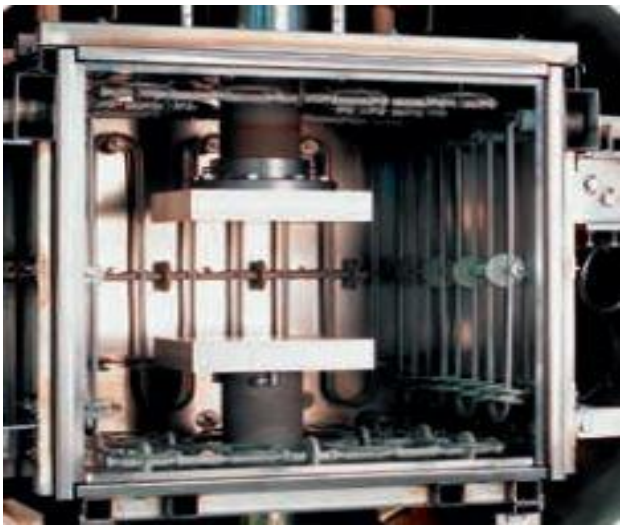

Figure 7. The diffusion bonding resistance heated

In this study, the diffusion bonding experiments are performed at two stages of screening and optimization based on the designed experiments which are presented in Tables 2 and 3, respectively. During bonding, the environment vacuum was set at 10^{-6} mbar and both heating and cooling rates are kept at 5 °C/s. To eliminate joining stress of the bonding operation and produce optimal structure, the bonded specimens were annealed at 400 °C for 1 h in vacuum furnace after the diffusion bonding process.

2.4. Tensile test

To measure the tensile strength of the diffusion bonded joints, tensile test specimens were machined according to the ASTM: E8/E8M-11 standard for tensile test. Figure 8 shows the schematic of the tensile test specimen prepared for this experiments.

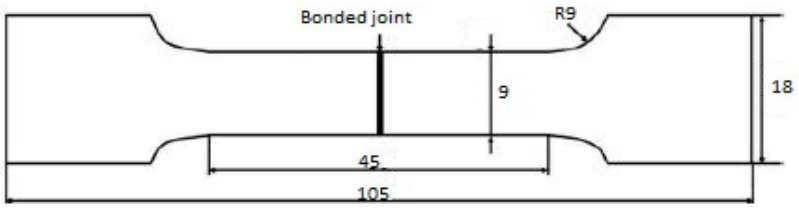

Figure 8. Schematic of the tensile test specimen

The tensile tests were performed by an insight model 5, produced by MTS Systems corp, Eden Prairie, MN with a constant strain rate of 0.5 mm/min. Figure 9 shows the universal testing machine.

Figure 9. Universal testing machine

2.5. Shear test

To measure the shear strength of the diffusion bonded joints, the shear test specimens were machined as per ASTM B831-11 standard. Figure 10 shows the schematic of the machined shear specimen. As tensile strength test, shear strength measurements of the shear test specimens of the diffusion bonded samples

are carried out using an insight model 5 universal testing machine as shown in Figure 9. The shear tests were performed at room temperature using custom made shear fixture with the crosshead speed of 1.8 mm/min.

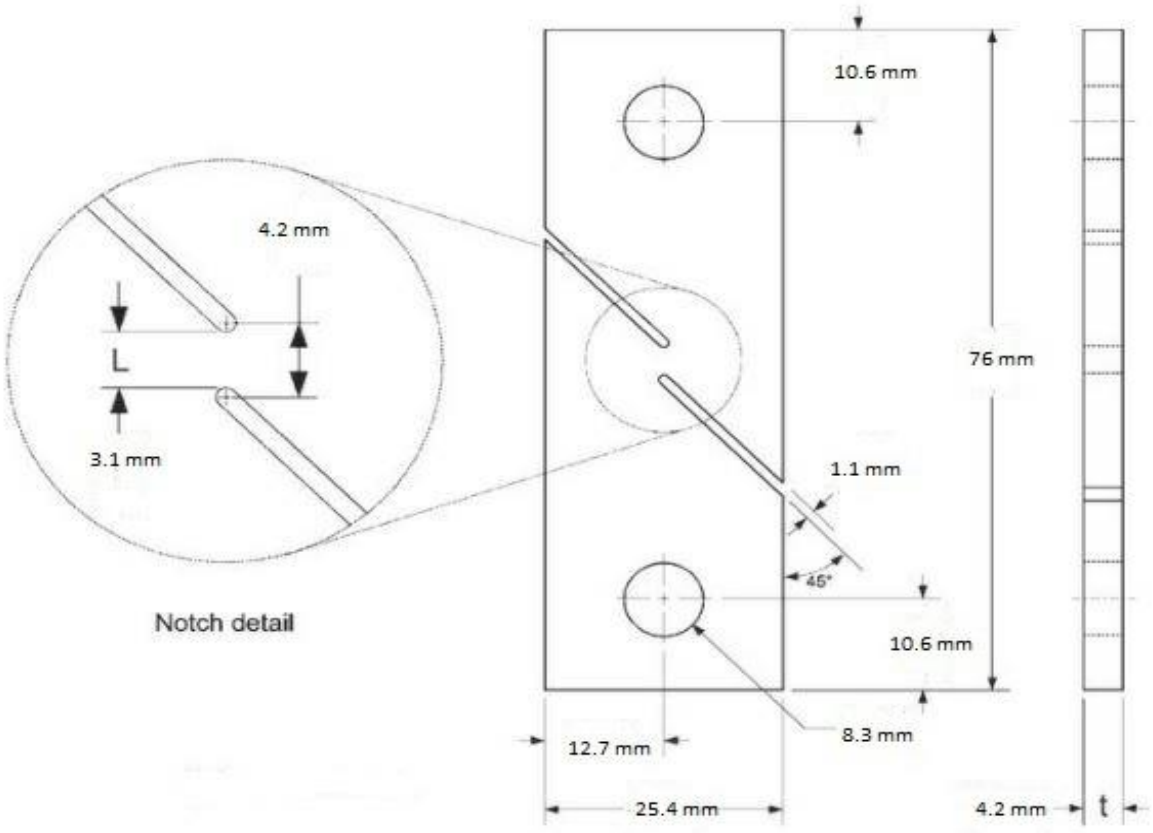

Figure 10. Schematic of the machined shear specimen

2.6. Microstructural examination

The microstructural examinations were conducted to evaluate the microstructural changes of the joints because of applied bonding pressures and temperatures and the relation between the achieved tensile and shear strength and the resulted microstructure. For microstructural examinations, specimens were sectioned from the diffusion-bonded joints, then the cross sectioned specimens were ground, polished,

and etched. Microstructural examinations of a few selective diffusions bonded samples near the interface of the joints were conducted using optical microscope (OM) and high resolution scanning electron microscopy (HR-SEM, Cam Scan 2300MV) in back-scattered (BSC) mode. The elemental chemical composition of the reaction layers at the interface cross section area of the specimen was analyzed through spot-wise analysis by means of an energy dispersive x-ray spectroscopy (EDS, Kevex). The diffusion of nickel content towards copper and towards the stainless steel 316 L side is evaluated from the analysis.

3. Results and discussion

3.1. DOE results

3.1.1. Screening experiments

First, 16 experiments were designed and performed for the screening stage (Table 2). The effects of 4 parameters of type of interlayer, bonding pressure, bonding temperature, and holding time on the mechanical behavior (tensile and shear strength) of dissimilar diffusion bonding (stainless steel of grade 316 L and pure copper (99.99 wt.%)) were investigated. The results obtained from the screening section (Table 2), revealed that the tensile and shear strength of the diffusion bonded joints where nickel was used as the interlayer were greater than the experiments performed without the interlayer. Figure 11 shows the main effect plots obtained from the screening experiments. In main effect plots, the slope of the lines has a direct relation with the effect of the parameter; i.e., the more the slope of the line, the more significant the parameter is [64]. Figure 11 (a) shows the effect of interlayer on the average tensile and shear strength of the bonded joints. As can be seen from the Figure 11, tensile and shear strength were improved by using nickel as the interlayer. The reason is attributed to the fact that interlayer reduces the chemical heterogeneity and thermodynamic instability in the joined zone and even prevent the thermal deformation [30, 50]. Effect of bonding pressure on the tensile and shear strength of the bonded joints is shown in Figure 11 (b). As it can be seen, the tensile and shear strength were enhanced as the pressure increased. It is attributed to the fact that pressure increases the contact area of the surfaces and reduces the voids by deformation of the contact area; therefore, strengthens the bonds (Will be further discussed in section 3.2.3) [1, 27, 50].

Figure 11 (c) shows the effect of bonding temperature on the tensile and shear strength of the bonded joints. The results shows that temperature has a significant effect on the tensile and shear strength of the bonded joints as compared to the other parameters (It has greater slope in comparison with other parameters). It can be seen that by raising the temperature, the tensile and shear strength is enhanced.

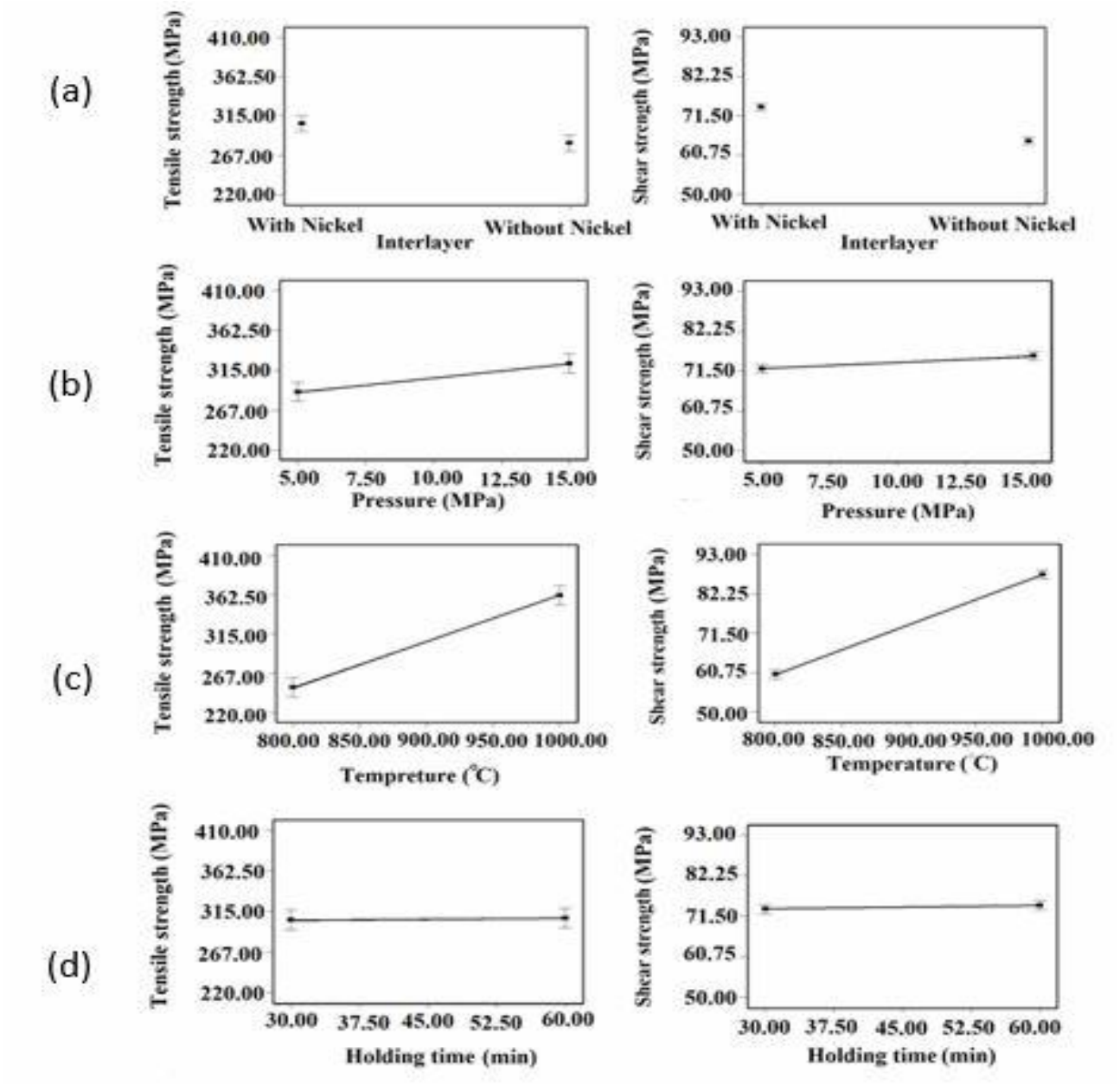

Figure 11. Main effect plots of screening section; (a) Effect of interlayer, (b) effect of bonding pressure, (c) effect of temperature, and (d) effect of holding time on the tensile and shear strength of the bonded joints

The reason is that increasing the bonding temperature, promotes the atomic diffusion of the chemical species and as a result increases the thickness of the reaction layer in the diffusion zone (will be further discussed in section 3.2.3) [48,70,84]. Figure 11 (d) illustrates the effect of holding time on the tensile and shear strength of the bonded joints that was performed in two time of 30 and 60 minutes. From this Figure, it can be concluded that holding time does not have significant effect on the tensile and shear strength because there is not any noticeable change in the slope of the lines in Figure 11 (d). It is obvious that longer holding times does not have any significant effect on the tensile and shear strength. The reason might be due to the fact that in this case, longer holding time (in the range that used in this research) did not enhance the atomic diffusion and contact area of the surfaces considerably [84]. Following equations show the coded models for tensile and shear strength of the bonded joints, which show the relation of each parameter on the tensile and shear strength of the bonded joints in the screening experiments.

$$Tensile\ strength = 294.31 - 11.81A + 16.81B + 55.56C + 1.06D \quad (1)$$

$$Shear\ strength = 69.25 - 4.63A + 1.75B + 13.63C + 0.50D \quad (2)$$

where, A, B, C, and D are interlayer, bonding pressure, bonding temperature, and holding time, respectively.

Eqs. (3) and (4) are the actual models of the tensile and shear strength using nickel as interlayer. Eqs. (5) and (6) are the actual models of tensile and shear strength without interlayer:

$$Tensile\ strength = -230.75000 + 3.36250 \times pressure + 0.55562 \times temperature + 0.070833 \times holding\ time \quad (3)$$

$$Shear\ strength = -53.75000 + 0.35000 \times pressure + 0.13625 \times temperature + 0.033333 \times holding\ time \quad (4)$$

$$Tensile\ strength = -254.37500 + 3.36250 \times pressure + 0.55562\ \times temperature + 0.070833 \times holding\ time \quad (5)$$

$$Shear\ strength = -53.75000 + 0.35000 \times pressure + 0.13625 \times temperature + 0.033333 \times holding\ time \quad (6)$$

The tensile and shear strength are obtained by setting the actual value of the pressure, temperature, and holding time in the Eqs. (3) to (6).

Eqs. (1) And (2) confirm that the effect of temperature is more than other parameters since the coefficient of temperature is more than other parameters. Bonding pressure is the second significant parameter after temperature while type of interlayer and holding time are less significant on the diffusion bonding process of stainless steel of grade 316 L and pure copper. The correlation coefficients for the tensile and shear strength models were calculated 0.95 and 0.99, respectively, which show that the experimental data and the models predicted values are fitted adequately.

3.1.2. Optimization experiments

Based on the results obtained from the screening experiments, and based on the Figure 11 and Eqs.(1) and (2), the parameters of bonding pressure and bonding temperature were selected as the significant parameters for further investigation in the optimization stage. Screening experiments also showed that tensile and shear strength are maximum while using nickel interlayer and holding time of 30 minutes (Figure 11 (a) and (d)). As a result, these two values were selected as constant parameters in the optimization step. Table 3 shows the CCD-RSM design of experiments as well as results obtained in the optimization step.

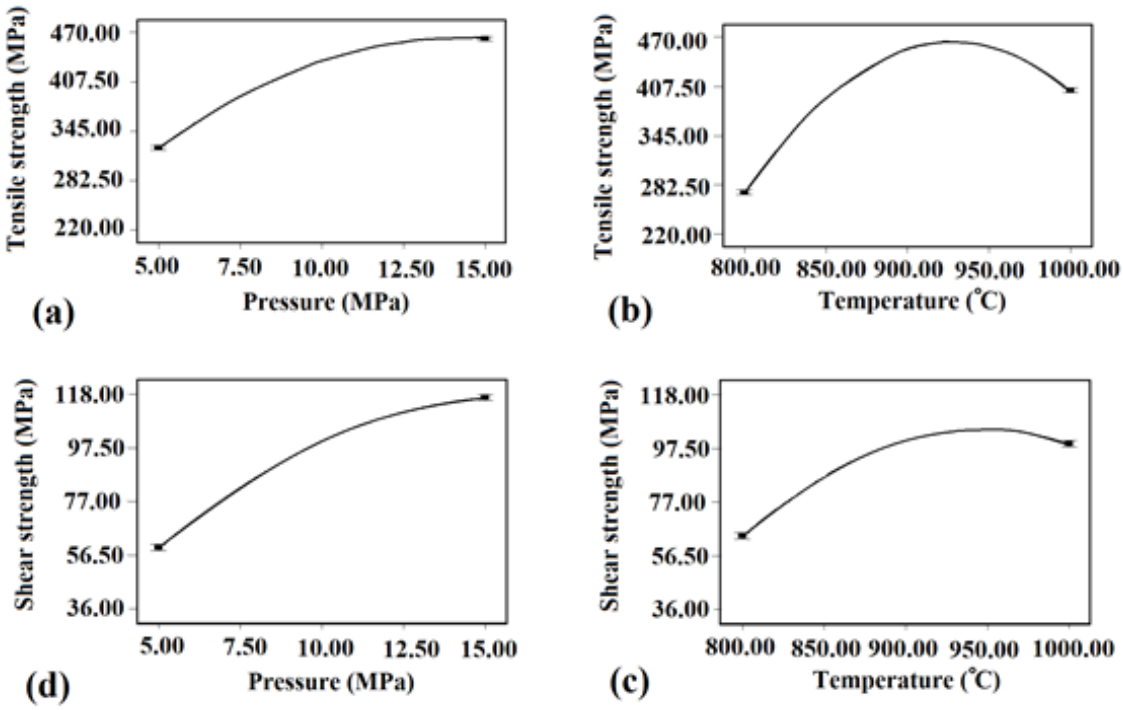

Figure 12. Effect of (a) pressure (Mpa) and (b) temperature (°C) on the tensile strength; and (c) temperature (°C) and (d) pressure on the shear strength

Based on the results obtained from the optimization step, several plots have been drawn. Figure 12 shows the main effect plots of pressure and temperature of the diffusion bonding process on the tensile and shear strength of the bonded joints. Figure 12 (a) demonstrates that tensile strength is enhanced from ca. 315 MPa to ca. 470 MPa as the pressure increases from 5 to 15 MPa. Figure 12 (b) shows that by increasing the temperature from 800 °C to ca.930 °C, the tensile strength is enhanced. However, further increase in temperature to 1000 °C leads to decrease in tensile strength. Figure 12 (c) displays increase in temperature form 800 °C to 960 °C bring about increase in shear strength from ca.58 MPa to 98 MPa. While further increase into the temperature leads to slight decrease/constant trend in the shear strength. Figure 12 (d) illustrates that by increasing in pressure from 5 to 15 MPa, shear strength is improved from ca. 57 MPa to ca.118 MPa. Due to the difference in intrinsic diffusion coefficients at the interface of two metals, voids would be created during diffusion bonding process. By increase in pressure not only the

voids are decreased but also plastic deformation take place in a way that enhances the contact of bond surface which leads to higher tensile and shear strength [70, 84]. Based on the aforementioned discussion, the interface contact rate increases, which improve the movement of atoms through this bonding, interface; therefore, more diffusion paths are created. There is no doubt on this fact that better diffusion occurs at higher temperatures which can be seen in the Figure 12 (b) and (c). However, with further increase in temperature tensile and shear strength decreases which is due to release of oxygen content at the interface of contact in high temperatures [85]. Besides, increase in diffusion bonding temperature promotes mass transfer of alloying elements across the interface, which is responsible for the increase in volume fraction of the reaction products and leads to more brittle joints (at higher temperature) [85].

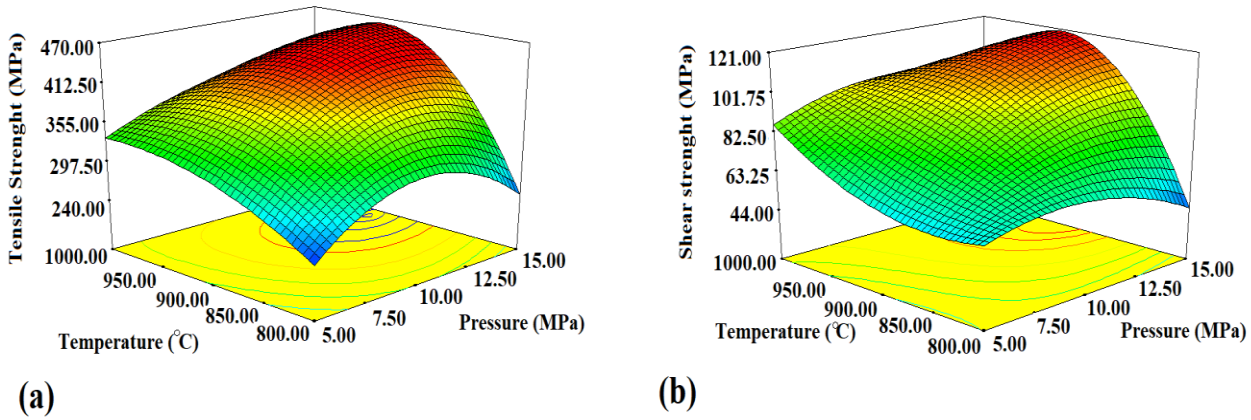

Figure 13. The 3D-surface diagram of (a) tensile and (b) shear strength as function of bonding temperature and pressure

Figure 13 demonstrates the 3D-surface diagrams of the tensile and shear strength as a function of bonding temperature and bonding pressure. Figure 13 shows the results shown in Figure 12 in another way in which pressure and temperature are both involved. It can be seen that except the main effects of both parameters on the tensile and shear strength; they have interactive influence on the tensile and shear

stress as well; i.e., change in one parameter affect the other parameter as well. It should be noted that the red area represents the highest values of tensile, shear strength; however, the blue area shows the lower amount of tensile, and shear strength. Based on the Table 2 and to optimize the influential parameters in diffusion bonding processes of joining stainless steel 316 L and pure copper, a number of experiments were done. Multiple regression analysis was used to obtain an numerical model for the diffusion bonding process and to maximize the tensile and shear strength of the bonded joints and following equations were obtained:.

$$Tensile\ strength = +429.80 + 68.24A + 36.42B + 15.25AB - 47.34A^2 - 76.34B^2 + 24.83A^2B - 49.49AB^2 \quad (7)$$

$$Shear\ strength = +100.60 + 28.99A + 18.34B + 4.00AB - 11.93A^2 - 18.92B^2 - 31.49AB^2 \quad (8)$$

Where A and B are bonding pressure and temperature, respectively. The correlation coefficient (R^2) for these models were calculated to be 0.9997 (for tensile strength) and 0.999 (for shear strength) which, indicating both models fit adequately to the experimental data. Table 4 shows analysis of variance (ANOVA) for the tensile strength. The model F-value of 2737.69 that is more than the minimum required F-value for this model (4.876) implies that the predicted model is significant. In addition, the p-values of less than 0.05 indicate that the model terms are significant [63]. Therefore, it is apparent from this table that A, B, AB, A^2, B^2, A^2B, and AB^2 are significant model terms. The "lack of fit p-value" should be more than 0.05 to prove that the model is significant. The lack of fit for this model is 0.0587 that is more than 0.05 proving that the lack of fit is not significant. If the lack of fit is significant it means that the model is not fitted to the experimental values [63].

Source	Sum of Squares	Degree of Freedom	Mean Square	F-Value	p-Value	
Model	91698.84	7	13099.83	2737.69	<0.0001	Significant
A-Pressure	18624.50	1	18624.50	3892.27	<0.0001	
B-Temperature	5304.50	1	5304.50	1108.57	<0.0001	
AB	930.25	1	930.25	194.41	<0.0001	
A^2	15588.44	1	15588.44	3257.77	<0.0001	
B^2	40538.53	1	40538.53	8472.00	<0.0001	
A^2B	1233.46	1	1233.46	257.78	<0.0001	
AB^2	4897.69	1	4897.69	1023.55	<0.0001	
Residual	23.92	5	4.78			
Lack of Fit	15.12	1	15.12	6.87	0.0587	Not significant
Pure Error	8.80	4	2.20			
Cor Total	91722.77	12				

Table 4. The analysis of variance table of the tensile strength model

Moreover, the correlation coefficient for this model (Eq. (7)) is ca. 1 (0.9997) that proves the model is fitted adequately to the experimental values. Table 5 demonstrates the analysis of variance for the shear strength model. As mentioned for the tensile strength model, also in this model the F-value of 1007.48 which more than the minimum required F-value (4.284) and the p-values of less than 0.05 imply the fact that the model and the model terms (A, B, AB, A^2, B^2, and AB^2) are significant. Moreover, similar to the tensile strength model the “lack of fit p-value” is not significant justifying that the model is fitted to the

experimental values. The correlation coefficient of ca. 1 (0.999) also indicate that the model fits well to the experimental data.

Source	Sum of Squares	Degree of Freedom	Mean Square	F-Value	p-Value	
Model	9265.88	6	1544.31	1007.48	<0.0001	Significant
A-Pressure	3362.00	1	3362.00	2193.30	<0.0001	
B-Temperature	2690.50	1	2690.00	1755.23	<0.0001	
AB	64.00	1	64.00	41.74	0.0007	
A^2	989.26	1	989.26	645.37	<0.0001	
B^2	2491.52	1	2491.52	1625.41	<0.0001	
AB^2	1983.41	1	1983.41	1293.94	<0.0001	
Residual	9.20	6	1.53			
Lack of Fit	4.00	2	2.00	1.54	0.3197	Not significant
Pure Error	5.20	4	1.30			
Cor Total	9275.08	12				

Table 5. The analysis of variance table of the shear strength model

Figure 14 shows the predicted optimum condition (bonding temperature and bonding pressure) for the diffusion bonding process of stainless steel of grade 316 L and pure copper to reach the maximum tensile and shear strength of the bonded joints using design expert 7 software from the analyzed data. The lines show the range of the parameters and the red points represent the exact values of the parameters at the optimum condition. As shown in the Figure 14 at the optimum condition of 14.03 (MPa) bonding

pressure and 925.21 (°C) bonding temperature (using nickel interlayer and 30 minutes holding time), 463.01 MPa tensile strength and 118.85 MPa shear strength can be reached.

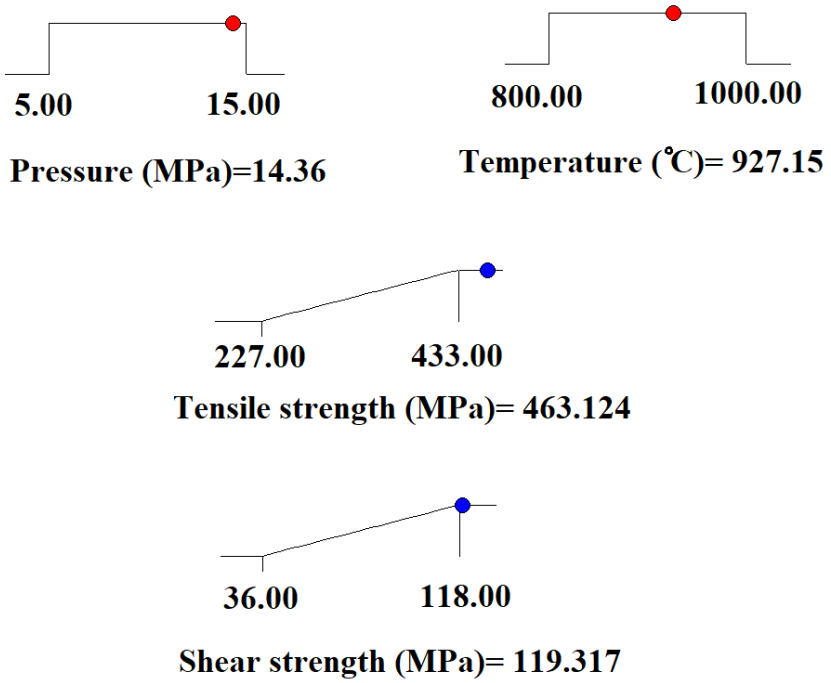

Figure 14. The optimum condition of pressure and temperature

The predicted optimum condition was tested for 3 times and the average tensile and shear strength were obtained 462.87 MPa and 119.23 MPa, respectively which confirm the replicability of the results. Figure 15 and 16 demonstrate the contour plots of the tensile and shear strength of the bonded joints. Contour plots are an alternative for 3D-surface diagrams shown in Figure 16; however, counter plots are more convenient and easier to interpret [63]. In the presented contour plots, each line shows a significant value of tensile or shear strength that can be obtained at different values of bonding temperatures and pressures. The last line in both tensile and shear strength diagrams shows the proposed optimum condition.

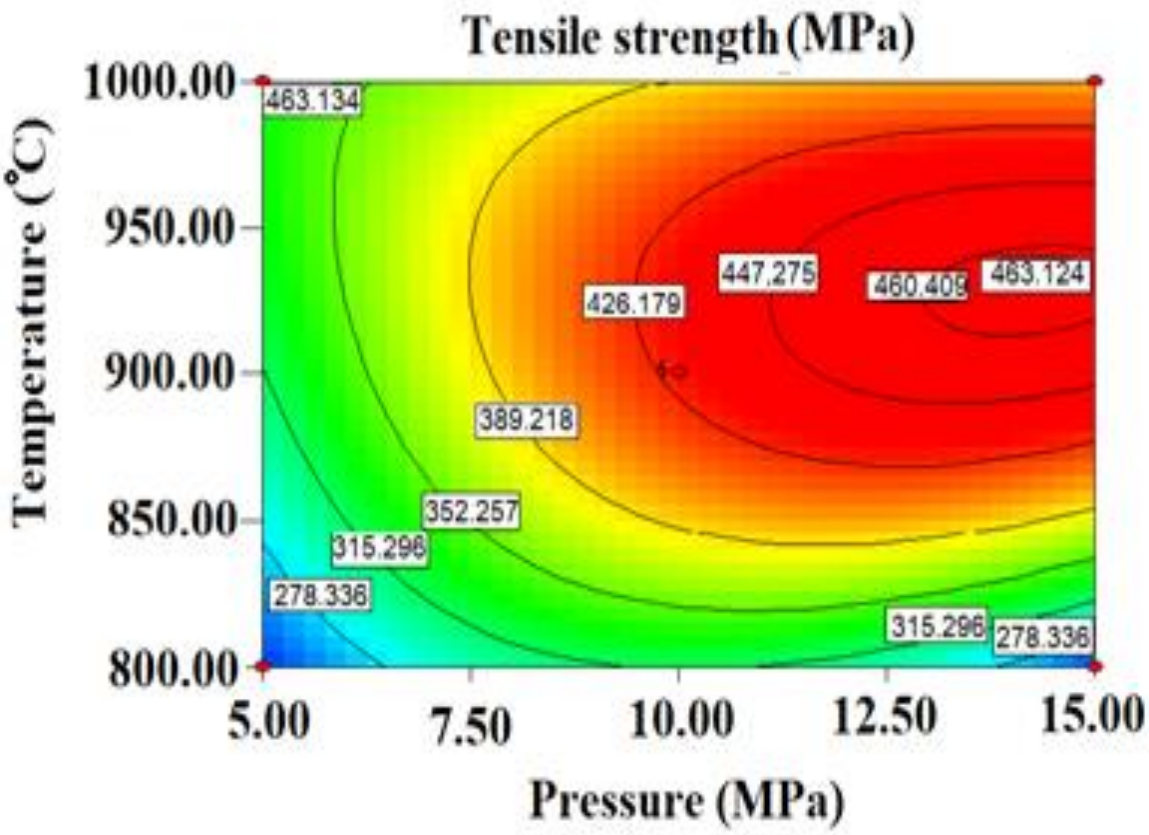

Figure 15. The contour plot of tensile strength

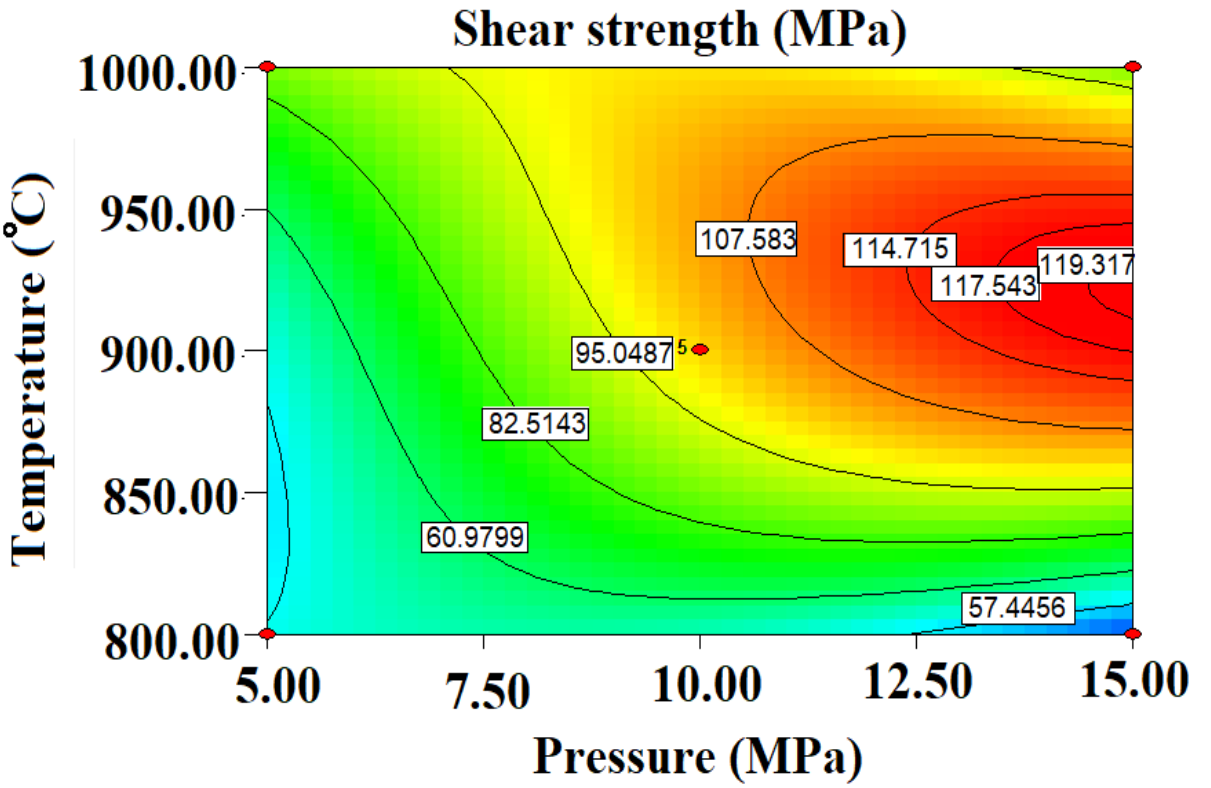

Figure 16. The contour plot of shear strength

3.2. Mechanical properties of the joints

3.2.1. Tensile strength

The tensile strength values of the various diffusion-bonded joints produced at different experimental conditions are plotted in Figure 17 it can be observed that the tensile strength is improved in sample 4 as compared to sample 3, which is due to the higher bonding pressure. The tensile strength value of sample 8 is better than sample 7 as a reason of higher bonding temperature. Although the bonding temperature is reduced in sample 9, the tensile strength is enhanced rather than sample 8 due to the thermal stresses at the bonding interfaces, which may be caused by the mismatch of thermal expansion coefficient of two dissimilar materials during cooling period.

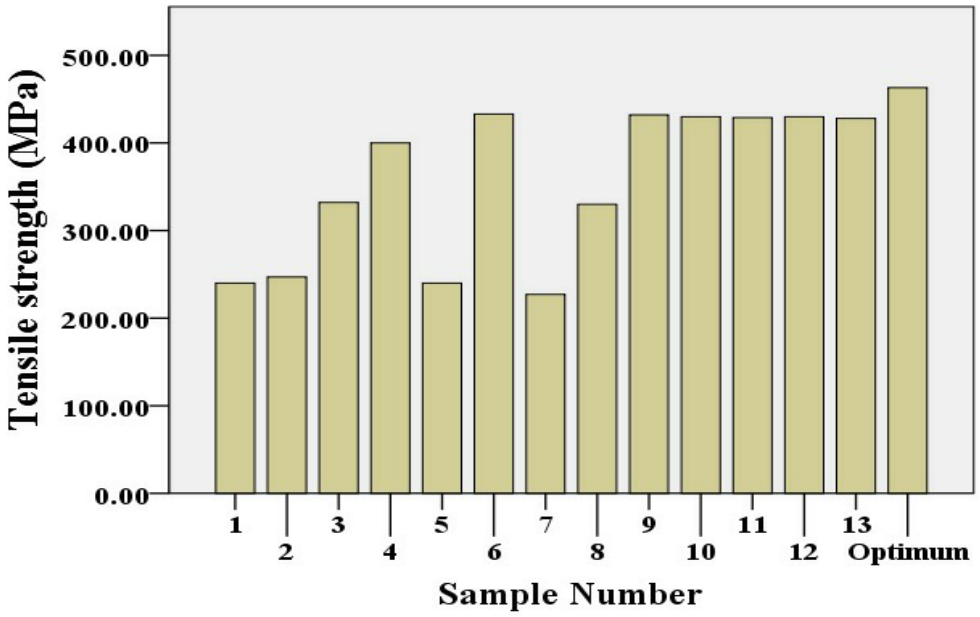

Figure 17. Tensile strength value (Mpa) of the corresponding samples

3.2.2. Shear strength

Figure 18 shows the Shear strength of the bonded joints at the performed experiments. Diffusion bonding of samples with similar temperatures and higher-pressure bonding have exhibited higher shear strength as shown in Figure 18. For example, from the shear strength measurement, it can be seen that diffusion bonding of stainless steel of grade 316 L and pure copper in sample 4 has better shear strength than sample 3. The shear strength value of the sample 8, which was prepared at higher temperature, is better in shear strength as compared to sample 7. However, in the case of samples 8 and 9, it stands out that although temperature is decreased, shear strength is enhanced. It should be noted that, the maximum shear strength value of 119.317 MPa is related to the optimum sample.

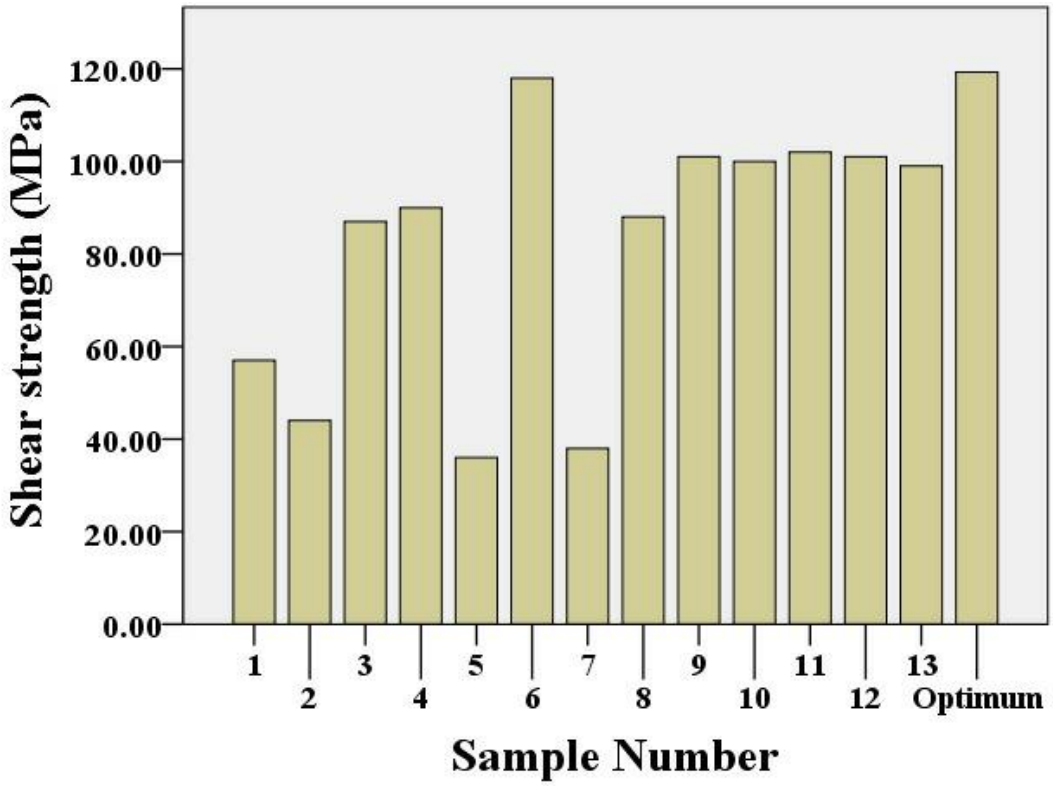

Figure 18. Shear strength value (MPa) of the corresponding samples

3.2.3. Investigation of temperature and pressure bonding on the diffusion bonding process

The diffusion bonding process can be classified into three stages [25, 26]. At the first stage, the applied bonding pressure deforms the course surfaces prior to heating which increases the contact area. At the second stage, the softer surface (Cu at the Ni–Cu interface and Ni at the SS–Ni one) deforms by raising temperature, which leads to removing of the gaps and cause well-suited contact of the surfaces. Eventually, the diffusion of atoms at constant temperature strengthens the bond and finishes the bonding process. It is obvious that bonding pressure plays a significant role at the first stage of the bonding process while bonding temperature is more influential parameter at the third stage. It is worth to mention that the second stage is the product of combination of pressure and temperature bonding. As mentioned before, pressure increases the contact area of the separated surfaces and at the same time reduces the voids by deformation of the contact area; therefore, strengthens the bonds. Figure 19 (a) and (b) provides the tensile and shear strength values of the bonded joints at the temperature bonding of 900 °C and pressure bonding of 2.93 MPa (sample 5), 10 MPa (sample 9), and 17.07 MPa(sample 6). The diagrams confirm that by raising the pressure, the tensile and shear strength of the bonded joints are enhanced.

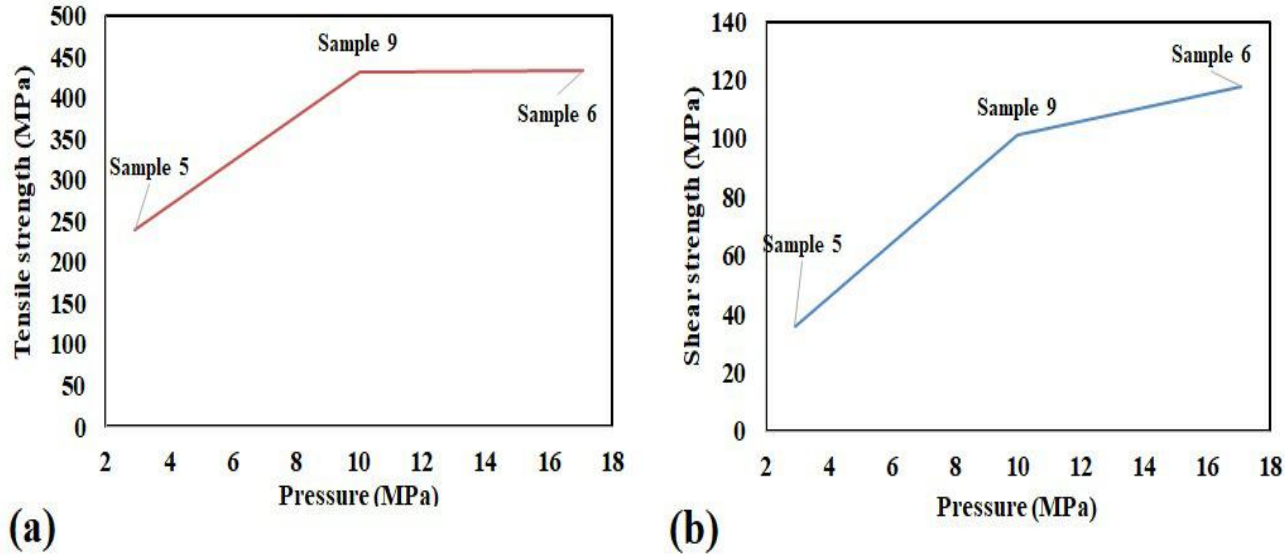

Figure 19. (a) Tensile and (b) shear strength values of the bonded joints with similar temperature bonding of 900 °C as a function of bonding pressure

Figure 20 ((a) and (b)) provide the tensile and shear strength values of the bonded joints with similar pressure bonding (10 MPa) as a function of bonding temperature. At low bonding temperature of 758.58 °C (sample 7), the tensile and shear strength are minimum. Due to the low thermal excitation of the atoms and limited diffusion of chemical species at this joining temperature the bonds are weak. By increasing the bonding temperature, the atomic diffusion of the chemical species is promoted that increases the thickness of the reaction layer in the diffusion zone. The enhancement of diffusion mass transfer at 1041.42 °C (sample 8) and 900 °C (sample 9) results in stronger atomic bonding with respect to 758.58 °C processing temperatures. Temperature is an effective parameter both in deformation of the surfaces and diffusion of the atoms in the diffusion bonding process. However, in higher bonding temperatures the thermal stresses occurred at the bonding interfaces. These stresses might be as a result of the mismatch of thermal expansion coefficient of two dissimilar materials during cooling period. The thermal stresses severely deteriorate the bond strength that could be the reason of decreasing the tensile and shear strength

at 1041.42 °C in comparison with 900 °C. The other factor that weaken the tensile and shear strength at 1041.42 °C, is the higher volume fraction of brittle intermetallic in the diffusion zone which overbalances the gain in strength due to the increased atomic thermal excitation [84].

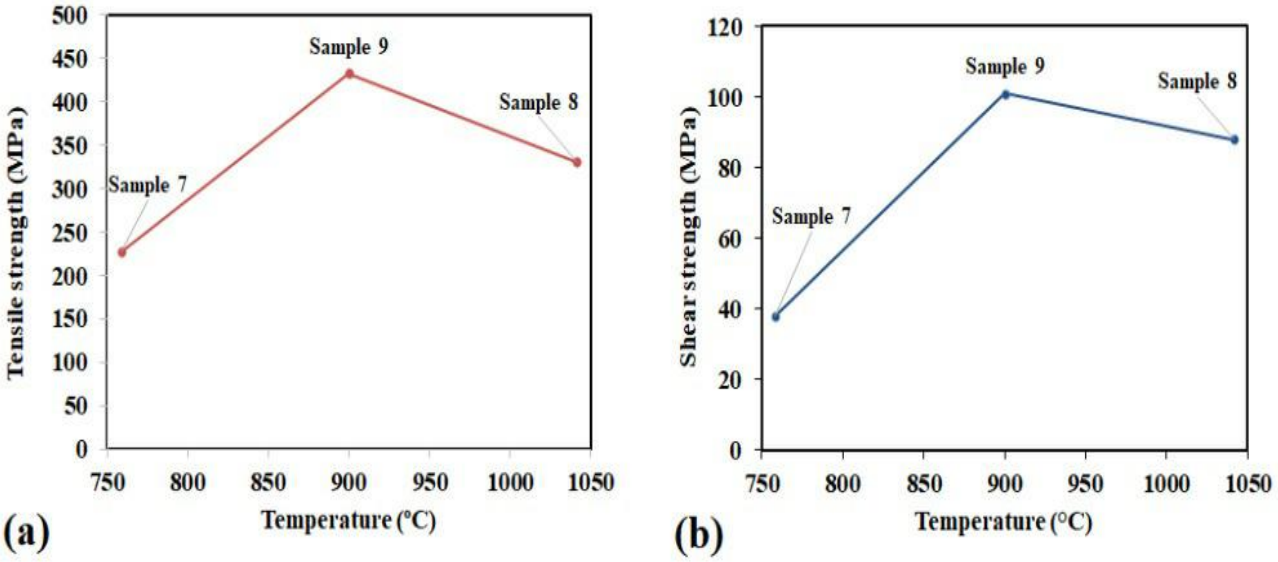

Figure 20. Tensile and shear strength values of the bonded joints with similar pressure bonding (10 Mpa) as a function of bonding temperature

3.2.4. Microstructural examination

3.2.4.1. Optical microscopy

The optical structure of the bonded joints were investigated using optical microscope. Figure 21 shows the optical microscopy images of the joint diffusion area. It can be seen from the images that there is an amount of inter-diffusion between the nickel interlayer and both of the substrates. Moreover, the joints are sufficiently sound, and there are low porosities in both substrate interfaces. From Figure 21 (b), it can be observed that there is a thin planar diffusion layer in stainless steel–nickel bonding interface planar.

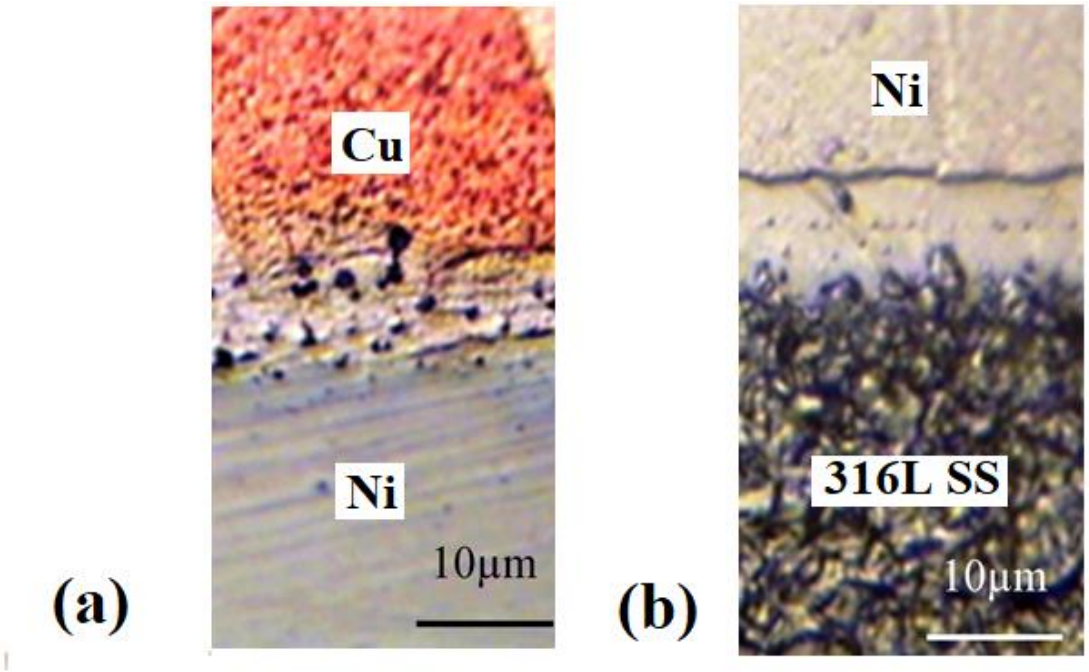

Figure 21. Optical microstructure of the optimum diffusion bonded joint (bonding temperature of 927.15 °C and bonding pressure of 14.36 MPa), (a) Cu-Ni interface, (b) Ni-SS interface

3.2.4.2. Scanning electron microscopy

Figure 22 illustrates the SEM-BSE of copper-nickel (interlayer) at 800 °C (sample 2), 900 °C (sample 9), 927.15 °C (optimum sample), respectively. Figure 23 provides the SEM-BSE of stainless steel grade of 316 L-nickel (as interlayer) at 800 °C (sample 2), 900 °C (sample 9), and 927.15 °C (optimum sample), respectively.

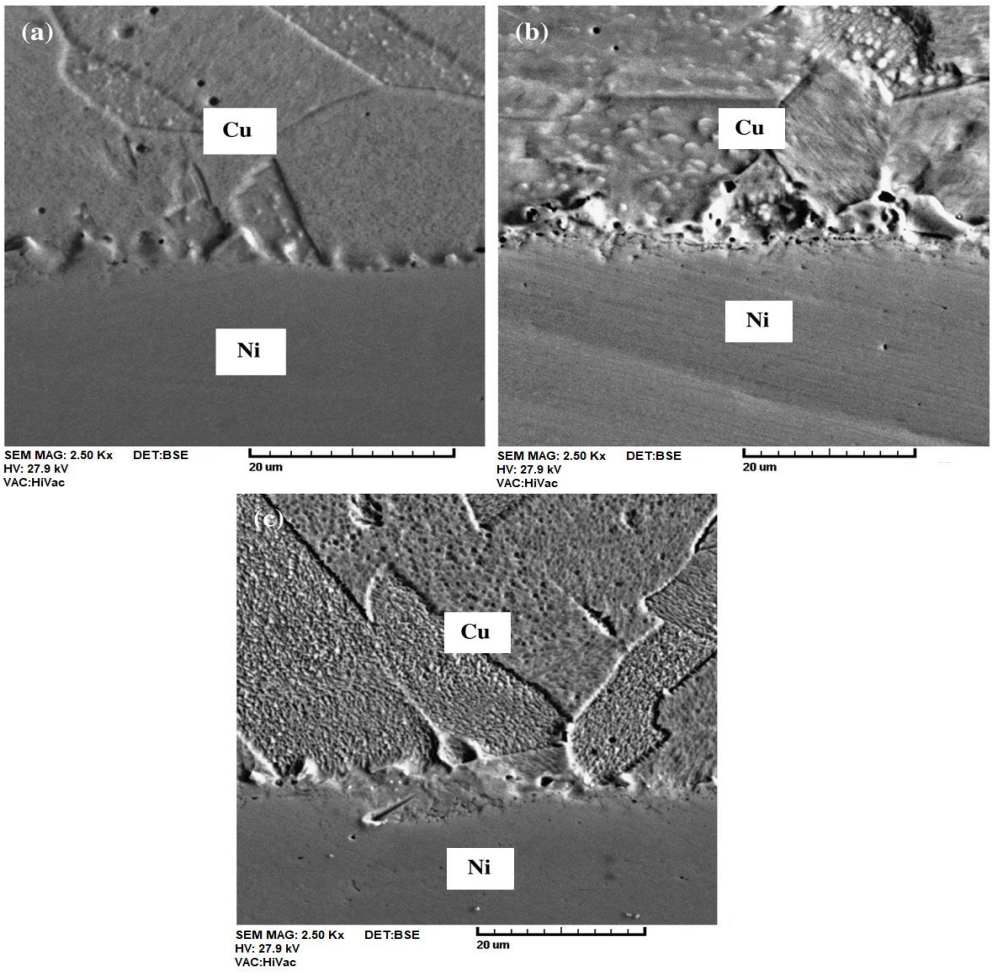

Figure 22. The SEM-BSE images of copper-nickel interface at temperature of: (a) 800 °C (sample 2), (b) 900 °C (sample 9), and (c) 927.15 °C (optimum sample)

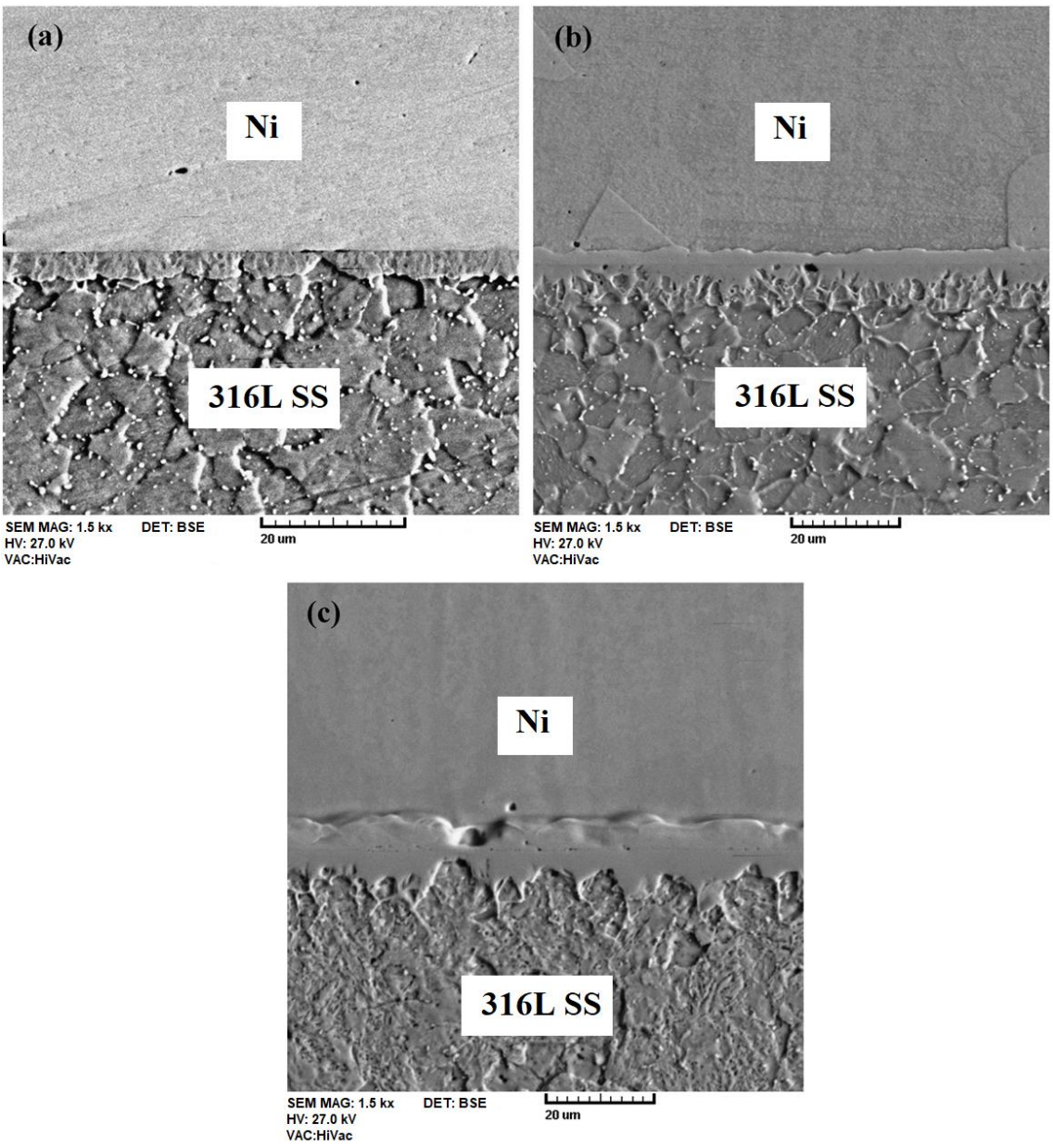

Figure 23. The SEM-BSE images of stainless steel-nickel interface at temperature of: (a) 800 °C (sample 2), (b) 900 °C (sample 9), and (c) 927.15 °C (optimum sample)

As shown in Figures 22 and 23 by increasing the temperature from 800 °C to about 927 °C the diffusion of nickel in copper and stainless steel grade of 316 L is increased. The following equation shows the Arrhenius equation:

$$D = D_0\ exp\ exp\left(-\frac{Q}{RT}\right) \rightarrow lnD = lnD_0 - \frac{Q}{RT} \quad (9)$$

Where, D_0 is diffusion constant ($\frac{m^2}{s}$), Q is the activation energy for diffusion ($\frac{kJ}{mol}$), R is real gas constant (8.314 $\frac{J}{mol}$), and T is the bonding temperature (K). Eq. (9) shows the positive effect of temperature on the diffusion; i.e., by increase in temperature the diffusion of nickel in copper and stainless steel grade of 316 L will be enhanced. Actually, the process temperature affects both the material yield stresses and the rate of atomic diffusion. These two parameters dictate the homogeneity of composition and the joint microstructure. The copper flowability is increased at the higher temperatures (800–1000 °C) as a reason of approaching the melting point. As it can be observed from Figures 22 and 23, the total diffusion area at the copper–nickel interface is larger than the nickel-stainless steel interface. This phenomenon occurs based on the greater tendency of atomic diffusion from the copper and stainless steel sides to the nickel side in comparison with the opposite direction. From Figures 22 and 23, it can be observed that at all experimental temperatures the micro-voids and porosities are visible in nickel–copper interfaces. In the case of stainless steel grade of 316 L and nickel interface, dark irregularly-shaped micro-voids are present at higher experimental temperatures, which are only observed at higher magnifications. Figure 24 shows the SEM-BSE images of stainless steel grade of 316 L-nickel and nickel-copper interfaces at temperature of 1041.42 °C (sample 8). As it can be seen in Figure 24 (b), in the nickel–copper interface, copper is a faster-diffusing species, which creates a large number of vacancies in its matrix.

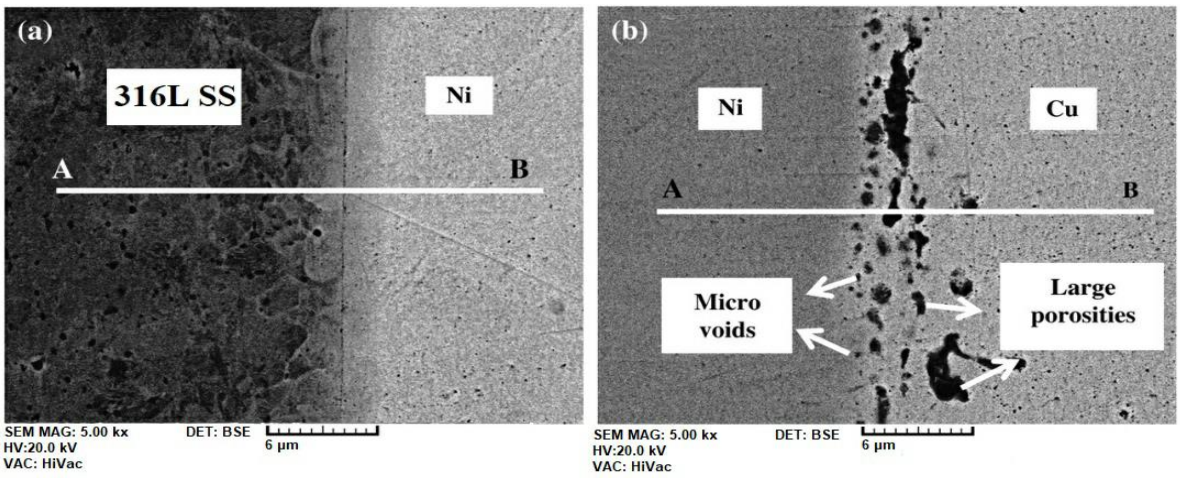

Figure 24. The SEM-BSE images of stainless steel grade of 316 L-nickel and nickel-copper interfaces at temperature of 1041.42 °C (sample 8)

The intrinsic diffusion coefficients of copper, nickel, alpha iron (α-Fe), and gamma iron (γ-Fe) at 900 °C, are provided in Table 6. The intrinsic diffusion coefficients of copper and alpha iron are greater than those of nickel and gamma iron. These differences produce a flux imbalance across the interfaces, which result in voids creation. The volume fraction of voids is further increased at higher bonding temperatures. Consequently, the generated discontinuities may thus play a major role in lowering the bond strength at 1041.42 °C processing temperature (sample 8). Previous studies on similar materials have concluded the same trend of Kirkendall void creation within diffusion-bonded interfaces [49, 86, 87].

Element	Intrinsic diffusion coefficient (m^2/s)
Copper	5×10^{-14}
Nickel	3×10^{-17}
Alpha iron	5×10^{-15}
Gama iron	3×10^{-17}

Table 6. The intrinsic diffusion coefficients of copper, nickel, alpha iron (α-Fe), and gamma iron (γ-Fe) at 900 °C [52, 53]

3.2.4.3. Study on the inter-diffusion of the atoms using EDS analysis

The inter-diffusion of iron, chromium, nickel and copper species have been demonstrated by EDS analysis. The SEM-BSE image and concentration profiles of the abovementioned elements in the interface area of the bonded joints at 800 °C (sample 2), 900 °C (sample 9), and 927.15 °C (optimum sample) are demonstrated in Figures 25, 26, and 27, respectively. It can be concluded that nickel only diffuses in a shorter distance into the stainless steel and copper sides in comparison with iron, chromium (from steel) and copper diffusion into the nickel side. In other words, the depth of diffusion for iron, chromium and copper atoms into the nickel side is greater than the opposite side. The penetration curves of the chemical species exhibit a gradual change in concentration profiles. As it is obvious in the line profiles close to the stainless steel side, chromium enrichment occurs for the bonded couples processed in the temperature range of 800–927 °C. With an increase in bonding temperature, the thickness of this layer significantly increases.

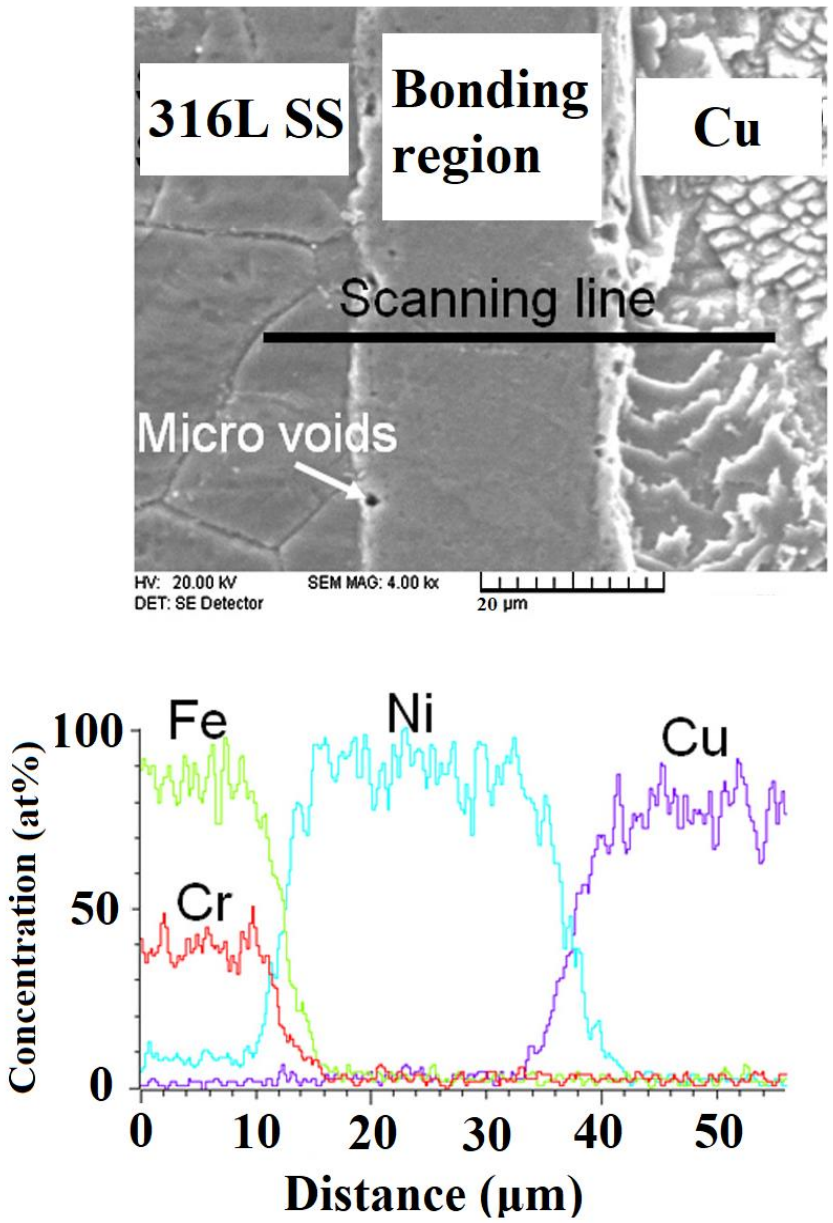

Figure 25. The SEM-BSE image and concentration profiles of iron, chromium, nickel and copper in the interface area of the bonded joints at 800 °C (sample2)

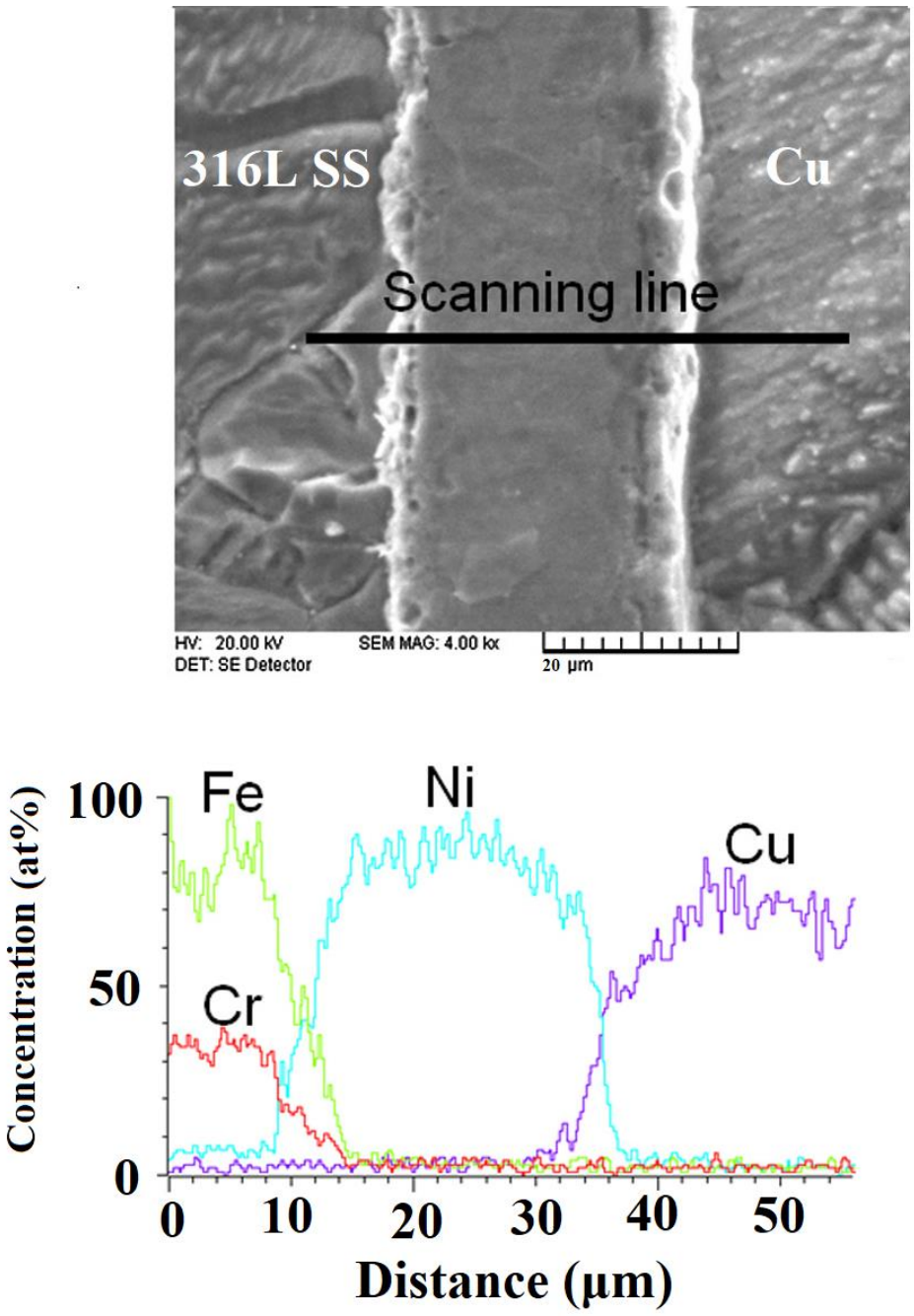

Figure 26. The SEM-BSE image and concentration profiles of iron, chromium, nickel and copper in the interface area of the bonded joints at 900 °C (sample9)

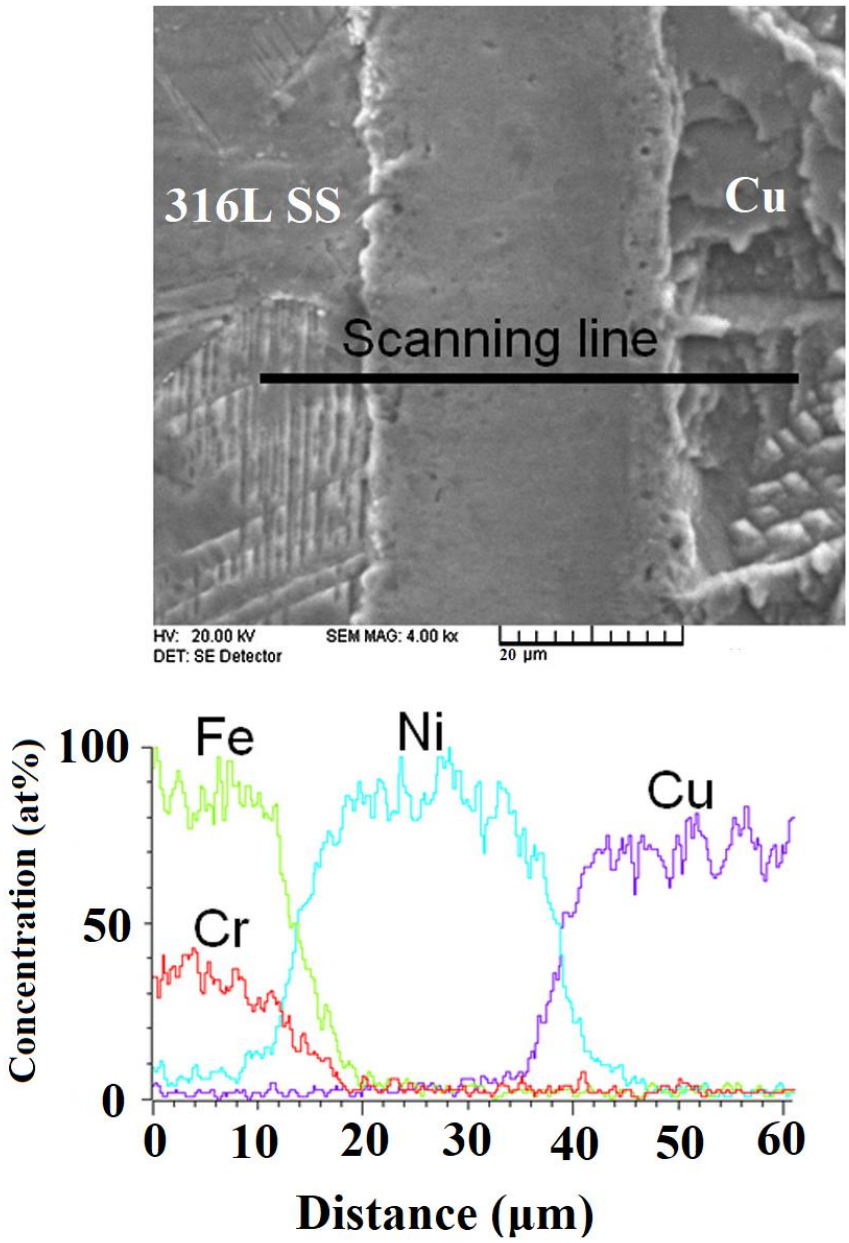

Figure 27. The SEM-BSE image and concentration profiles of iron, chromium, nickel and copper in the interface area of the bonded joints at 927.15 °C (optimum sample)

4. Conclusions

Stainless steel and copper combination have many industrial applications due to the beneficial properties of the bimetal. This type of combination has an increasing demand in automobile, rail, and aviation industry. Although the combination of stainless steel and copper alloys is of great importance in industrial productions, achievement of this joint become a challenging task due to their obvious mismatches, such as thermomechanical properties, physical properties and chemical properties [48]. 316 L is a molybdenum containing grade; in which, molybdenum improves austenitic stability and corrosion resistance through the martensitic transformation stage. In addition, this stainless steel have great formability, ductility, and austenitic stability. Due to these properties, a special CERN specification covered this grade to reduce difficulties of the LHC interconnections [58]. Also, copper is the most applicable metal in heat fluxes of diverter because of the good conductivity and thermal stress resistance [53]. According to the aforementioned discussion, in this thesis, the diffusion bonding of stainless steel of grade 316 L and pure copper (99.99 wt.%) was evaluated. The experiments were performed at two stages of screening and modification to investigate the effect of interlayer, bonding pressure, bonding temperature, and holding time on the tensile and shear strength of the bonded joints. At the screening stage 16 experiments were designed using factorial design and conducted to determine the most effective parameters of the diffusion bonding and the following results have been concluded:

- The samples that were joined using nickel interlayer had more tensile and shear strength alongside the samples joined without interlayer due to the reduction of chemical heterogeneity and thermodynamic instability in the joined zone and prevent of thermal deformation in the samples with nickel interlayer.

- By increasing the bonding pressure, the tensile and shear strength were enhanced as a result of increasing the contact area of the surfaces and reducing the voids in higher bonding pressures.
- Raising the temperature enhanced the tensile and shear strength since in higher temperatures, the atomic diffusion is enhanced.
- The longer holding time does not have significant effect on the tensile and shear strength in the performed period of time (30 minutes and 60 minutes) due to the possibility that there was not considerable enhance in the atomic diffusion and contact area of the surfaces.

According to the screening results, the bonding pressure and temperature were further investigated at the modification stage as the experiments variables and the two parameters of nickel interlayer and holding time (30 minutes) were considered constant in this stage. The CCD design, a subdivision of response surface methodology (RSM) were used to design 13 experiments and the following results have been achieved:

- Increase in pressure from 5 to 15 MPa leads to higher tensile and shear strength since the voids are decreased and plastic deformation takes place in a way that enhances the contact of bond surface.
- By increasing the temperature from 800 to ca. 930 °C, the tensile and shear strength of the joint bonds were enhanced due to the increase in the diffusion of the atoms. However, above ca. 930 °C, the tensile and shear strength were decreased by raising the temperature to 1000 °C. This phenomenon happened due to the reason that with further increase in temperature, the release of oxygen content at the interface of the contact and the promotion of the mass transfer of alloying elements across the interface lead to increase in the volume fraction of the reaction products. This also can cause more brittle joints (at higher temperature). Also in higher bonding temperatures the thermal stresses occurred at the bonding interfaces, which made as a result of the mismatch of thermal expansion coefficient of two dissimilar materials during cooling period, weaken the bonds strengths.

- The optimum condition was determined as 14.03 (MPa) bonding pressure and 925.21 (°C) bonding temperature (using nickel interlayer and 30 minutes holding time). The tensile strength of 463.01 MPa and shear strength of 118.85 MPa can be reached at the optimum condition.
- The SEM-BSE images of both copper-nickel and stainless steel 316 L-nickel at 800 °C (sample 2), 900 °C (sample 9), 927.15 °C (optimum sample) confirms that by increasing the temperature from 800 °C to about 927 °C the diffusion of nickel in copper and stainless steel grade of 316 L is increased as a result of promotion in atomic diffusions.
- The SEM-BSE image nickel-copper interfaces at temperature of 1041.42 °C (sample 8) confirms that in the nickel–copper interface, copper is a faster-diffusing species, which creates a large number of vacancies in its matrix and weaken the bonds strengths.
- The inter-diffusion of iron, chromium, nickel and copper species have been demonstrated by EDS analysis at 800 °C (sample 2), 900 °C (sample 9), 927.15 °C (optimum sample) revealed that nickel only diffuses in a shorter distance into the stainless steel and copper sides in comparison with iron, chromium and copper diffusion into the nickel side. In other words, the depth of diffusion for iron, chromium and copper atoms into the nickel side is greater than the opposite side.

5. References

[1] J. Zhang, Y. Huang, Y. Liu, Z. Wang, Direct diffusion bonding of immiscible tungsten and copper at temperature close to Copper's melting point, Mater. Des. 137 (2018) 473–480.

[2] C.L. Bauer, G.G. Lessmann, Metal-joining methods, Annu. Rev. Mater. Sci. 6 (1976) 361–387.

[3] C.W. INSPECTOR, American Welding Society, (1968).

[4] K. Weman, Welding processes handbook, Elsevier, 2011.

[5] T.W. Eagar, The physics of arc welding processes, in: Adv. Join. Technol., Springer, 1990: pp. 61–68.

[6] J. Elmer, Standardizing the art of electron-beam welding, Lawrence Livermore Natl. Lab. Retrieved. (2008) 10–16.

[7] S. Schiller, U. Heisig, S. Panzer, Electron beam technology, John Wiley & Sons, 1982.

[8] C.L.M. Cottrell, Electron beam welding—a critical review, Mater. Des. 6 (1985) 285–291.

[9] P. Asadi, K. Kazemi-Choobi, A. Elhami, Welding of magnesium alloys, in: New Featur. Magnes. Alloy., InTech, 2012.

[10] R.P. Martukanitz, A critical review of laser beam welding, in: Crit. Rev. Ind. Lasers Appl., International Society for Optics and Photonics, 2005: pp. 11–25.

[11] L. Reclaru, C. Susz, L. Ardelean, Laser beam welding, Timisoara Med J. 60 (2010) 86–89.

[12] R.D. Adams, Adhesive bonding: science, technology and applications, Elsevier, 2005.

[13] M. Wiemer, C. Jia, M. Toepper, K. Hauck, Wafer bonding with BCB and SU-8 for MEMS

packaging, in: Electron. Syst. Technol. Conf. 2006. 1st, IEEE, 2006: pp. 1401–1405.

[14] R.F. Wolffenbuttel, Low-temperature intermediate Au-Si wafer bonding; eutectic or silicide bond, Sensors Actuators A Phys. 62 (1997) 680–686.

[15] M.M. Schwartz, Brazing, ASM international, 2003.

[16] G. Humpston, D.M. Jacobson, Principles of soldering, ASM international, 2004.

[17] S.H. Carpenter, R.H. Wittman, Explosion welding, Annu. Rev. Mater. Sci. 5 (1975) 177–199.

[18] H.A. Mohamed, J. Washburn, Mechanism of solid state pressure welding, (1975).

[19] D. Lingnau, Method of solid state welding and welded parts, (2003).

[20] J.P. Bergmann, F. Petzoldt, R. Schürer, S. Schneider, Solid-state welding of aluminum to copper—case studies, Weld. World. 57 (2013) 541–550.

[21] F. Findik, Recent developments in explosive welding, Mater. Des. 32 (2011) 1081–1093.

[22] S.A.A. Akbari-Mousavi, L.M. Barrett, S.T.S. Al-Hassani, Explosive welding of metal plates, J. Mater. Process. Technol. 202 (2008) 224–239.

[23] J. Banker, B. Craig, Titanium: A Solution for Highly Corrosive Hydrometallurgical Applications-Alloy Selection, Cladding and Fabrication, in: Proc. ALTA 2009 Nickel-Cobalt Conf., 2009.

[24] A. Elrefaey, W. Tillmann, Solid state diffusion bonding of titanium to steel using a copper base alloy as interlayer, J. Mater. Process. Technol. 209 (2009) 2746–2752.

[25] D.J. Stephenson, Diffusion bonding 2, Springer Science & Business Media, 2012.

[26] N.F. Kazakov, Diffusion bonding of materials, Elsevier, 2013.

[27] N. Kurgan, Investigation of the effect of diffusion bonding parameters on microstructure and mechanical properties of 7075 aluminium alloy, Int. J. Adv. Manuf. Technol. 71 (2014) 2115–2124.

[28] N.F. KAZAKOV, Diffusion bonding of materials((Book)), Moscow/Oxford, Mir Publ. Press. 1985, 304. (1985).

[29] C.S. Lee, H. Li, R.S. Chandel, Vacuum-free diffusion bonding of aluminium metal matrix composite, J. Mater. Process. Technol. 89 (1999) 326–330.

[30] G.M. Zeer, E.G. Zelenkova, Y.P. Koroleva, A.A. Mikheev, S. V Prokopy'ev, Diffusion bonding through interlayers, Weld. Int. 27 (2013) 638–643.

[31] S. Chen, F. Ke, M. Zhou, Y. Bai, Atomistic investigation of the effects of temperature and surface roughness on diffusion bonding between Cu and Al, Acta Mater. 55 (2007) 3169–3175.

[32] H. Mehrer, Diffusion in solids: fundamentals, methods, materials, diffusion-controlled processes, Springer Science & Business Media, 2007.

[33] R.W. Balluffi, J.W. Cahn, Mechanism for diffusion induced grain boundary migration, Acta Metall. 29 (1981) 493–500.

[34] A.A. Shirzadi, H. Assadi, E.R. Wallach, Interface evolution and bond strength when diffusion bonding materials with stable oxide films, Surf. Interface Anal. An Int. J. Devoted to Dev. Appl. Tech. Anal. Surfaces, Interfaces Thin Film. 31 (2001) 609–618.

[35] S. Dunkerton, D.J. Stephenson, Diffusion bonding, TWI World Cent. Mater. Join. Technol. (1991) 1–5.

[36] A. Joseph, S.K. Rai, T. Jayakumar, N. Murugan, Evaluation of residual stresses in dissimilar weld

joints, Int. J. Press. Vessel. Pip. 82 (2005) 700–705.

[37] R.L. Klueh, J.F. King, J.L. Griffith, Simple test for dissimilar-metal welds., Weld. J. 62 (1983) 154.

[38] C.D. Lundin, Dissimilar metal welds-transition joints literature review, Weld. J. 61 (1982) 58–63.

[39] J.R. Davis, Hardfacing, weld cladding, and dissimilar metal joining, ASM Int. ASM Handbook. 6 (1993) 789–829.

[40] R.L. Klueh, The effect of carbon on 2.25 Cr-1 Mo steel:(I). Microstructure and tensile properties, J. Nucl. Mater. 54 (1974) 41–54.

[41] R.K.S. Raman, Role of microstructural degradation in the heat-affected zone of 2.25 Cr-1Mo steel weldments on subscale features during steam oxidation and their role in weld failures, Metall. Mater. Trans. A. 29 (1998) 577–586.

[42] R.L. Klueh, J.F. King, Austenitic stainless steel-ferritic steel weld joint failures., Weld. J. 61 (1982) 302.

[43] R.W. Emerson, W.R. Hutchinson, Welded joints between dissimilar metals in high temperature service, Weld. J. 31 (1952) 126s-141s.

[44] B.K.G. Dutta, A.G. Dhingra, R.G. Chhibber, Evaluation of Residual Stresses in Bimetallic Welds, (2010).

[45] R.A. Swift, H.C. Rogers, Embrittlement of 2⅟ 4Cr-1Mo steel weld metal by postweld heat treatment, Weld. J. 52 (1973).

[46] R. Bruscato, Embrittlement of 21/4Cr-1 Mo Weld Deposits, Weld. J. 49 (1970) 148S-156S.

[47] D.L. Olson, ASM handbook: welding, brazing, and soldering, Asm Intl, 1993.

[48] X. Yuan, K. Tang, Y. Deng, J. Luo, G. Sheng, Impulse pressuring diffusion bonding of a copper alloy to a stainless steel with/without a pure nickel interlayer, Mater. Des. 52 (2013) 359–366.

[49] S. Kundu, S. Chatterjee, Characterization of diffusion bonded joint between titanium and 304 stainless steel using a Ni interlayer, Mater. Charact. 59 (2008) 631–637.

[50] E. Akca, A. Gürsel, The importance of interlayers in diffusion welding-A review, Period. Eng. Nat. Sci. 3 (2015).

[51] K.N. Chen, C.S. Tan, A. Fan, R. Reif, Morphology and bond strength of copper wafer bonding, Electrochem. Solid-State Lett. 7 (2004) G14–G16.

[52] X.F. Ang, A.T. Lin, J. Wei, Z. Chen, C.C. Wong, Low temperature copper-copper thermocompression bonding, in: Electron. Packag. Technol. Conf. 2008. EPTC 2008. 10th, IEEE, 2008: pp. 399–404.

[53] R.K. Roy, S. Singh, M.K. Gunjan, A.K. Panda, A. Mitra, Joining of 304SS and pure copper by rapidly solidified Cu-based braze alloy, Fusion Eng. Des. 86 (2011) 452–455.

[54] K. Banerjee, S.J. Souri, P. Kapur, K.C. Saraswat, 3-D ICs: A novel chip design for improving deep-submicrometer interconnect performance and systems-on-chip integration, Proc. IEEE. 89 (2001) 602–633.

[55] K.N. Chen, A. Fan, C.S. Tan, R. Reif, Temperature and duration effects on microstructure evolution during copper wafer bonding, J. Electron. Mater. 32 (2003) 1371–1374.

[56] T.H. Kim, M.M.R. Howlader, T. Itoh, T. Suga, Room temperature Cu–Cu direct bonding using surface activated bonding method, J. Vac. Sci. Technol. A Vacuum, Surfaces, Film. 21 (2003)

449–453.

[57] A. Fan, A. Rahman, R. Reif, Copper wafer bonding, Electrochem. Solid-State Lett. 2 (1999) 534–536.

[58] S. Agosteo, M. Silari, EUROPEAN ORGANISATION FOR NUCLEAR RESEARCH EUROPEAN LABORATORYFOR PARTICLEPHYSICS, (2001).

[59] C. Garion, B. Skoczeń, S. Sgobba, Constitutive modelling and identification of parameters of the plastic strain-induced martensitic transformation in 316 L stainless steel at cryogenic temperatures, Int. J. Plast. 22 (2006) 1234–1264.

[60] C.J. Guntner, R.P. Reed, The effect of experimental variables including the martensitic transformation on the low temperature mechanical properties of austenitic stainless steels, Trans. ASM. 55 (1962) 399–419.

[61] K. Couturier, S. Sgobba, Phase stability of high manganese austenitic steels for cryogenic applications, 2000.

[62] C. Yao, B. Xu, X. Zhang, J. Huang, J. Fu, Y. Wu, Interface microstructure and mechanical properties of laser welding copper–steel dissimilar joint, Opt. Lasers Eng. 47 (2009) 807–814.

[63] M.J. Anderson, P.J. Whitcomb, DOE simplified: practical tools for effective experimentation, Productivity press, 2016.

[64] R. Golmohammadzadeh, F. Rashchi, E. Vahidi, Recovery of lithium and cobalt from spent lithium-ion batteries using organic acids: Process optimization and kinetic aspects, Waste Manag. 64 (2017) 244–254.

[65] A.A. Negemiya, S. Rajakumar, V. Balasubramanian, Diffusion bonding of a titanium alloy to

austenitic stainless steel using copper as an interlayer, SN Appl. Sci. 1 (2019) 1128.

[66] K. Meng, Y. Zhang, Z. Zhang, Diffusion bonding of low carbon steel and pure zirconium with Cu-base amorphous interlayer, J. Mater. Process. Technol. 262 (2018) 471–478.

[67] V. Srikanth, A. Laik, G.K. Dey, Joining of stainless steel 304L with Zircaloy-4 by diffusion bonding technique using Ni and Ti interlayers, Mater. Des. 126 (2017) 141–154.

[68] K.P. Singh, R. Bhavsar, K. Patel, S.S. Khirwadkar, A. Patel, K. Bhope, Joining of WCu-CuCrZr coupon materials by diffusion bonding technique for divertor plasma facing components, Fusion Eng. Des. 121 (2017) 272–281.

[69] K. Hongchao, G. Heng, W. Jun, T. Bin, L. Jinshan, Diffusion bonding between Zr-based metallic glass and copper, Rare Met. Mater. Eng. 45 (2016) 42–45.

[70] K.P. Singh, A. Patel, K. Bhope, S.S. Khirwadkar, M. Mehta, Optimization of the diffusion bonding parameters for SS 316 L/CuCrZr with and without Nickel interlayer, Fusion Eng. Des. 112 (2016) 274–282.

[71] G. Pardal, S. Ganguly, S. Williams, J. Vaja, Dissimilar metal joining of stainless steel and titanium using copper as transition metal, Int. J. Adv. Manuf. Technol. 86 (2016) 1139–1150.

[72] C. Velmurugan, V. Senthilkumar, S. Sarala, J. Arivarasan, Low temperature diffusion bonding of Ti-6Al-4V and duplex stainless steel, J. Mater. Process. Technol. 234 (2016) 272–279.

[73] S. Wang, Y. Ling, J. Wang, G. Xu, Microstructure and mechanical properties of W/Cu vacuum diffusion bonding joints using amorphous Fe–W alloy as interlayer, Vacuum. 114 (2015) 58–65.

[74] S. Zakipour, M. Samavatian, A. Halvaee, A. Amadeh, A. Khodabandeh, The effect of interlayer thickness on liquid state diffusion bonding behavior of dissimilar stainless steel 316/Ti-6Al-4V

system, Mater. Lett. 142 (2015) 168–171.

[75] Q. Cai, W. Liu, Y. Ma, H. Liu, Microstructure, residual stresses and mechanical properties of diffusion bonded tungsten–steel joint using a V/Cu composite barrier interlayer, Int. J. Refract. Met. Hard Mater. 48 (2015) 312–317.

[76] B. Szwed, M. Konieczny, Influence of diffusion bonding parameters on the structure and properties of titanium and stainless steel joints with copper interlayer, J. Achiev. Mater. Manuf. Eng. 67 (2014) 21–25.

[77] K. Aydın, Y. Kaya, N. Kahraman, Experimental study of diffusion welding/bonding of titanium to copper, Mater. Des. 37 (2012) 356–368.

[78] H. Lee, J. Yoon, J. Yoo, Y. Yi, A study on diffusion bonding of steel and copper alloy, Materwiss. Werksttech. 42 (2011) 985–989.

[79] H. Sabetghadam, A.Z. Hanzaki, A. Araee, Diffusion bonding of 410 stainless steel to copper using a nickel interlayer, Mater. Charact. 61 (2010) 626–634.

[80] J. Xiong, Q. Xie, J. Li, F. Zhang, W. Huang, Diffusion bonding of stainless steel to copper with tin bronze and gold interlayers, J. Mater. Eng. Perform. 21 (2012) 33–37.

[81] G. Mahendran, V. Balasubramanian, T. Senthilvelan, Developing diffusion bonding windows for joining AZ31B magnesium and copper alloys, Int. J. Adv. Manuf. Technol. 42 (2009) 689–695.

[82] S. Kundu, M. Ghosh, A. Laik, K. Bhanumurthy, G.B. Kale, S. Chatterjee, Diffusion bonding of commercially pure titanium to 304 stainless steel using copper interlayer, Mater. Sci. Eng. A. 407 (2005) 154–160.

[83] M. Eroglu, T.I. Khan, N. Orhan, Diffusion bonding between Ti-6Al-4V alloy and microduplex

stainless steel with copper interlayer, Mater. Sci. Technol. 18 (2002) 68–72.

[84] H. Nishi, T. Araki, M. Eto, Diffusion bonding of alumina dispersion-strengthened copper to 316 stainless steel with interlayer metals, Fusion Eng. Des. 39 (1998) 505–511.

[85] H. Soflaei, S.E. Vahdat, Microstructure study of diffusion bonding of centrifuged structural steel-bronze, Arch. Foundry Eng. 16 (2016) 99–104.

[86] O. Yilmaz, H. Celik, Electrical and thermal properties of the interface at diffusion-bonded and soldered 304 stainless steel and copper bimetal, J. Mater. Process. Technol. 141 (2003) 67–76.

[87] S. Kundu, S. Chatterjee, Diffusion bonding between commercially pure titanium and micro-duplex stainless steel, Mater. Sci. Eng. A. 480 (2008) 316–322.